Master's thesis

NTNU
Norwegian University of Science and Technology
Faculty of Engineering
Department of Geoscience and Petroleum

Abdul Ahad

Experimental Study for Wear Characteristics and Wear Prediction of Corrosion Resistant Alloy Material Tubulars

Master's thesis in Petroleum Engineering
Supervisor: Sigbjorn Sangesland
Co-supervisor: Bjorn Brechan
June 2022

NTNU
Norwegian University of
Science and Technology

Abdul Ahad

Experimental Study for Wear Characteristics and Wear Prediction of Corrosion Resistant Alloy Material Tubulars

Master's thesis in Petroleum Engineering
Supervisor: Sigbjorn Sangesland
Co-supervisor: Bjorn Brechan
June 2022

Norwegian University of Science and Technology
Faculty of Engineering
Department of Geoscience and Petroleum

NTNU
Norwegian University of
Science and Technology

Summary

Precise casing wear estimation is important to ensure appropriate well integrity and safer production of hydrocarbons. The amount of casing wear depends not only on operational parameters but also on the casing material. Experience from the Norwegian continental shelf (NCS) has proved that chrome material are subject to more wear as compared to carbon steel. 13% Cr materials are typically used where reservoir fluids are in contact with casing. However, some of the well construction techniques exposes 13% Cr materials to wear. In the NCS, multilateral wells where the contribution from each lateral is controlled, there is often a portion of 13% Cr material in the casing. Another frequently used technique involving wear of 13% Cr on the NCS wells is through tubing rotary drilling (TTRD).

The recent models for estimation of casing wear are valid for carbon steel but they fail to predict accurate wear for casings made of corrosion resistant alloy (CRA). Therefore, research was required to identify the reasons for the difference in wear characteristics of CRAs versus standard carbon steel.

A series of experiments were designed by analyzing data from NCS and tests were performed by varying the side force on 13Cr80 and 13CrS110 casings to investigate their wear characteristics. The experimental results revealed that wear estimation of chrome casings can be predicted. It was found that casings made from CRAs are subject to a different wear mechanism as compared to regular carbon steel. The research showed CRA material is prone to excessive wear depending on the side force. Furthermore, the contact pressure threshold for chrome casings has been established at low side force.

Acknowledgment

I wish to thank my supervisor Professor Sigbjorn Sangesland for giving me the opportunity to work on this topic under his supervision. I would like to express my gratitude to him for help and support.

It was immense pleasure to work with Mr. Bjorn Brechan as my co-supervisor. My kind appreciation goes to him for his support, valuable advices and technical guidance throughout this course work. I have benefited greatly from his knowledge and experience.

Abdul Ahad

31st May, 2022

NTNU, Trondheim

Table of Contents

List of Figures

List of Tables

Abbreviations

CRA:	Corrosion resistant alloys
NCS:	Norwegian continental shelf
CPT:	Contact pressure threshold
TTRD:	Through tubing rotary drilling
WF:	Wear factor
Fn:	Normal force
Ls:	Sliding distance
ODtj:	Outer diameter of tool joint
N:	Rotational speed
T:	Time
f:	Fraction of tool joint to drill string length
Ψ:	Work function
CF:	Correction Factor
WP:	Wear percent
OD:	Outer Diameter
ROP:	Rate of penetration
WOB:	Weight on bit
DLS:	Dogleg severity
MD:	Measured depth
DP:	Drill Pipe

1 Introduction

In modern time, the development of complicated wells has increased significantly with long horizontal wells, extended reach wells, multilateral and highly deviated wellbores. These complex wells demand good wellbore integrity. At the same time, these drilling operations can lead to casing wear problem. Casing wear is one of the important challenges experienced by the oil & gas industry. But accurate wear prediction is still ambiguous. Various researches and industry projects on casing wear estimation has been conducted which resulted in development of models. Efforts have been made to decrease the uncertainties of parameters and accurately predict wear. However, the accuracy of the models is questionable especially with respect to different casing materials. Field experience shows that the models are accurate for carbon steel material. But their application could not be accurately extended to casings with chrome material which exhibits a higher rate of wear as compared to predicted values for standard material. Therefore, casing material should be taken into account in order to accurately estimate casing wear.

Different casing materials will experience different wear rates. The fundamental casing wear model was developed by joint industry project DEA -42 (Maurer Engineering) after extensive laboratory experiments. This model was not made to predict wear characteristics for corrosion resistant alloys (CRA) casing material. DEA -42 performed more than 300 tests on standard steel material but did not incorporated 13% Cr material to their objective. The wear mechanism for chrome material is complex and it is difficult to predict their occurrence and effect. One of the ways to account these challenges is to change the wear factor in the casing wear equation. This is the practical and only option for the industry to predict wear for CRA materials.

In order to understand the wear characteristics of casings made from CRA, a number of TTRD wells from Norwegian continental shelf (NCS) were analyzed. Simulations were performed for each well using actual operational data to extract the side forces and design an appropriate test matrix. The experiments were performed on 13Cr80 and 13CrS110 casings by varying the side force from lowest 650 lb/ft to maximum 4300 lb/ft while keeping other parameters same.

The results from experiments demonstrated the concept of contact pressure threshold (CPT) and confirmed its existence at much lower side force for chrome casings as compared to standard

casing material. Wear characteristics of casings made up of CRAs has been established and improvements in current methodology of wear modelling has been suggested.

1.1 Objectives

The outlined research in this thesis is builds on work performed by Andreas Teigland (2021). A model for predicting wear for CRA materials was proposed in the work. However, only few tests were performed and the recommendation was to conduct more tests in a controlled environment such as proposed in API CW7 to build more confidence to the conclusion. Several aspects to be considered for further testing were:

- Contact Pressure Threshold (CPT): Does CRA materials have a CPT?
- TTRD is a frequent operation where CRA material is exposed to wear. What is the typical range of side forces experienced in these operations?
- Is there a difference in wear characteristics between 13Cr and 13CrS?
- Can the tests in the work of Andreas Teigland be replicated and the proposed model for prediction of wear of CRA material be confirmed?

2 Wear Theory

2.1 Casing Wear

Casing wear is removal of material from internal surface of casing due to mechanical work typically from tool joint while drilling. Wear can occur where the drill string is in contact with the casing either at tool joint or the pipe body. However, the pipe body contact with casing is minimal where the well has low dogleg severity, short or normal length drill pipe and at moderate side force. Therefore, wear due to pipe body rotation is often negligible. Tool joints are often the main point of contact between casing and drill pipe especially if the hardbanding is not flush. The rate of wear is directly related to the wear mechanism. There are three main types of wear mechanism that is *two body adhesive wear, two body abrasive wear* and *three body abrasive wear.* Two body adhesive wear is the dominant mechanism at high contact pressure. It is also known as *galling* which occurs when two bodies are in contact and welds are sheared off due to relative motion of the mating surfaces and metal is removed from casing. Two body abrasive wear is also known as *chipping* which occurs when sharp particles on tool joint, for instance hardfacing material cut into the casing material due to high local contact stress. Three body abrasive wear occurs when a tool joint and the casing surfaces are separated by solid particles such as barite or drill cuttings. This mechanism is also known as *grinding*. This can cause fatigue and embrittlement of metal which leads to micro fractures at the surfaces. This wear mechanism is dominant at low pressures [1].

White and Dawson (1987) proposed a casing wear model by assuming that casing wear is solely a result of the rotation of the drill pipe. This model stated, the volume removed relates to the energy dissipated by friction in the wear process. Later, a wear factor was introduced by Hall et al. (1994) as a slight modification of White and Dawson' model. The wear factors became an integral part of the casing wear model. It is based on the theory that when a tool joint rotates against the inner wall of the casing, a crescent shaped groove is worn into the inner surface. This model assumes that the volume of steel removed from each unit length of casing at a certain point of contact is proportional to frictional work done by the tool joint rotating in contact with the casing. This model was verified from the DEA-42 joint-industry project (Maurer Engineering 2000) by performing more than 300 laboratory tests. This work resulted in formulation of fundamental equation for casing wear estimation [2] [3] [5].

$$V = WF\,.Fn\,.\;Ls \qquad (1)$$

Where,

WF = Wear factor
Fn = Normal force
Ls = Sliding distance

An expression for sliding distance is given below:

$$Ls = \frac{ODtj\,.\,\pi\,.\,N\,.t\,.\,f}{60} \qquad (2)$$

Where,

ODtj = Outer diameter of tool joint
N = Rotational speed
t = Time
f = Fraction of tool joint to drill string length

The work function can be written as:

$$\psi = ODtj\,.\pi\,.N\,.t\,.f\,.Fn\,.60 \qquad (3)$$

Where,

Ψ = Work function
Fn = Normal force

Equation (1) can be expressed as:

$$V = WF\,.\psi \qquad (4)$$

The above equation (1) describes the linear relationship between wear volume and work done by the tool joint on casing surface. However, Williamson (1981) established that contact pressure is the appropriate parameter to be included in casing wear modelling rather than the contact load. Contact pressure varies during the wear process due to changes in the contact area between tool joint and casing which results in non-linear relationship between wear volume and work. Experimental data from Williamson's research shows that wear rates can be correlated with contact pressure. Hall and Malloy (2005) performed wear tests to verify the concept of contact pressure in accordance with Williamson's research. Hence, a new model for casing wear based on the previous model of (Hall et al. 1994) was developed which accounts the effect of contact pressure. Work

function is the product of the normal force and sliding distance. Hall and Malloy (2005) research revealed the non-linear relationship between wear volume and work function [2] [3].

$$V = A * (1 - e^{(-B*\psi^{C})}) \tag{5}$$

Where,

A, B, C = Empirical constants

ψ = Work function

Equation (5) shows that maximum wear volume equal to the value of the empirical constant A resulted in concept called the contact pressure threshold (CPT). The minimum contact pressure at which wear occurs is known as CPT. The DEA-42 project showed that the concept of contact pressure could be included in (Eq. 1) by varying the wear factor as a function of wear percent. The Wear percent (WP) is defined as the fraction of wall thickness lost to the original wall thickness. The wear factor decreases with increase in wear depth or wear percentage and reaches an asymptotic value for wear percentages greater than 40%. In order to account for the non-linearity of the wear characteristics, an empirical correction factor (CF) was introduced by (Mittal et al. 2019). The adjusted wear factor or non-linear wear factor is defined as the product of the original wear factor and a correction factor. It will be used to estimate the actual wear [2] [3] [4].

$$CF = \begin{cases} 7.0, & if\ WP < 1 \\ 1.0, & if\ WP < 50 \\ 0.878 + 6.122/WP & otherwise \end{cases} \tag{6}$$

2.2 Determination of Contact Pressure Threshold

Both wear factor and differential wear factor are required to determine the contact pressure threshold as illustrated in Fig 2.1. The conventional wear factor is found when plotting the wear volume against the wear function and defined as the slope of the line connecting the origin of the curve to the data point measured at the conclusion of wear test. The differential wear factor is the slope of the tangent to the curve at this point [6].

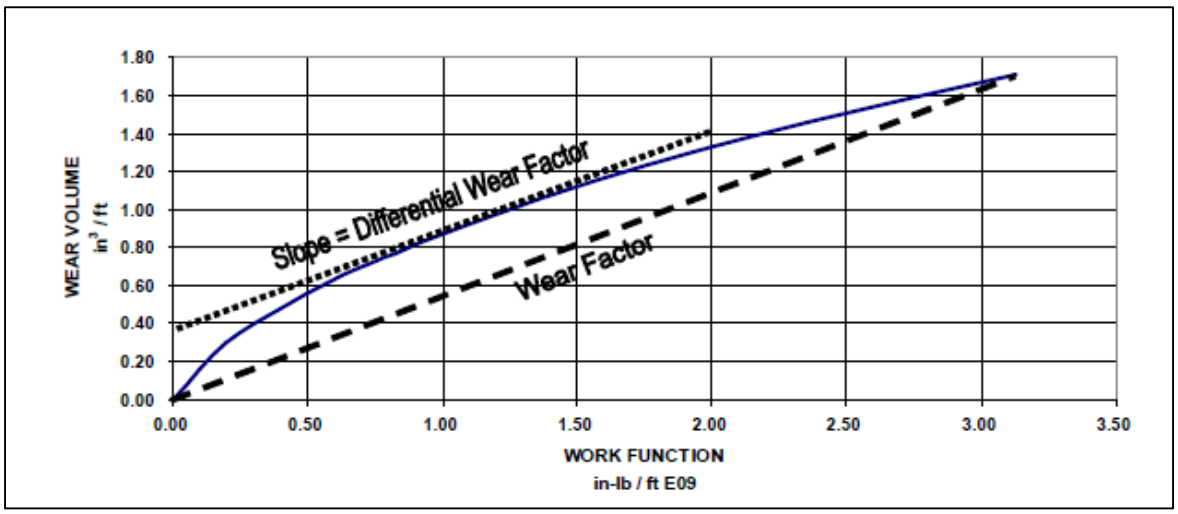

Fig 2.1: Wear Factor [6]

The conventional wear factor is expressed as;

$$WF(\Psi) = \frac{V(\Psi)}{\Psi} = \frac{A * (1 - e^{(-B*\Psi^C)})}{\Psi} \tag{7}$$

The differential wear factor is expressed as;

$$\delta WF(\Psi) = \frac{dV}{d\Psi} = A * B * C * e^{(-B*\Psi^C)} * \Psi^{(C-1)} \tag{8}$$

Contact pressure is defined as the lateral load divided by the projected area of the wear groove. In order to determine the contact pressure threshold, the wear factors are plotted as a functions of the contact pressure. First, the wear groove depth is plotted vs the work function. Then, data curve fitting is done which will provide an analytical expression for groove depth as shown in Fig 2.2. The relationship between the casing inside diameter, tool joint diameter, groove depth and groove width is illustrated in Fig 2.3. After determining the groove width, the projected area corresponding to each value of the groove depth is calculated. Now, by using the projected area and the lateral load, the contact pressure can be determined. The corresponding values of contact pressure and wear factors can be properly matched and plotted, since all of these quantities have the work function as a parameter [6].

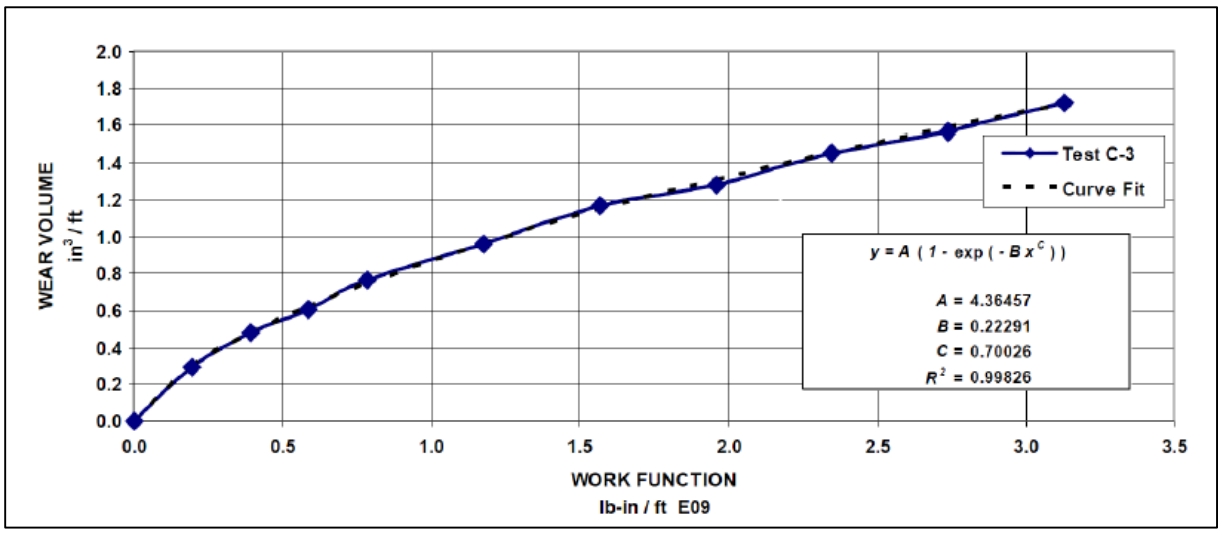

Fig 2.2: Non Linear Curve Fitting [6] [8]

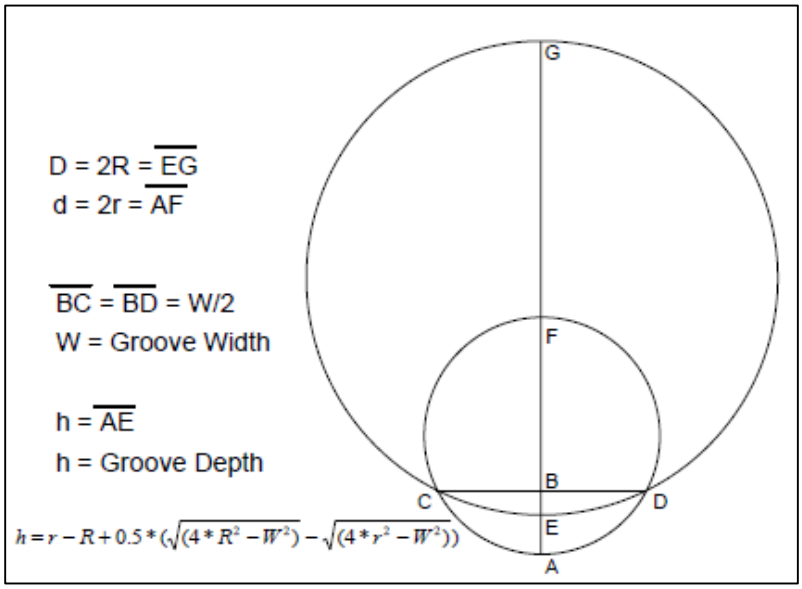

Fig 2.3: Relationship between Groove Depth and Groove Width [6]

Fig 2.4 shows how to determine the CPT. Plotting wear factor as a function of contact pressure reveals the CPT. It is the value where the conventional and differential wear factors converge at the abscissa [6].

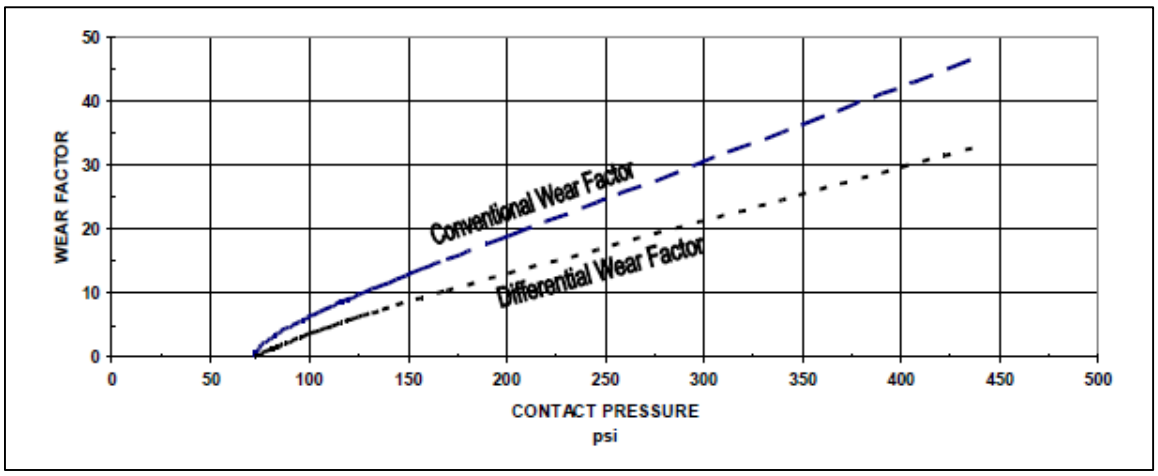

Fig 2.4: Wear factors vs Contact pressure [6]

The wear factor indicates the rate at which casing will wear, whereas contact pressure threshold provides an estimate of anticipated wear groove depth. Casing wear may be self-limiting, if the hardbanding material has low casing wear characteristics and at high contact pressure threshold. The higher the value of contact pressure threshold, the lower ultimate wear groove depth will be. This is shown in fig 2.5 [6].

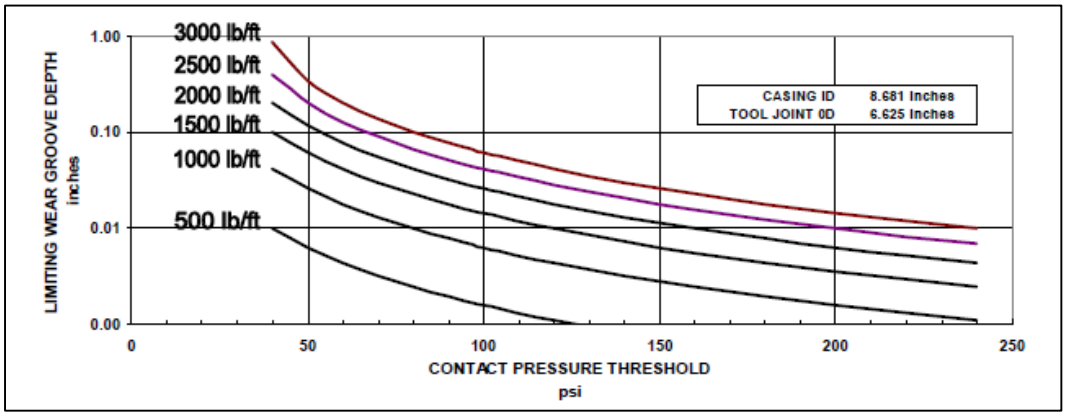

Fig 2.5: Wear Groove Depth vs Contact Pressure Threshold [6]

2.3 Wear Characteristics of Chrome material Casing

The casing wear equations presented above are valid for most of the tubulars made up of carbon steel material. However, tubulars of chromium material are associated with large and varying wear factors. Industry experience shows that chrome material casings are subject to more wear as compared to other materials. Sønstabø (2008) investigated wells on the Norwegian Continental

Shelf (NCS) and reported severe wall loss for L80Cr13 casing. The research established that the wear factor for L80Cr13 varied and it was difficult to predict final wall loss. Whereas wear factors were consistent for carbon steel and wall loss was predictable. This indicates a limitation and inability to model and predict wear characteristics of chrome casing. The wear factor is a parameter containing many uncertainties and it is generally back calculated from actual logged casing wear values. Sønstabø found that wear factors were consistent for the carbon steel section of the well but the wear factor varied significantly for the length with chrome material of the casing. Consequently, final integrity of the casing was poor. Kjellevold (2013) analyzed wells from the NCS and also reported poor correlation between simulated and logged wear for casing of chrome material. The research concluded that the modern casing wear estimation models are inappropriate for chrome materials [2] [3] [8].

Today's casing wear models build on the work done by DEA -42. They are based on empirical measurements made on standard steel material of casing. The dominant wear mechanisms are found to be adhesive and abrasive wear. However, CRA material is also subject to corrosive wear. The purpose of chromium material casings is to provide corrosion inhibitive properties and ignoring the effect of corrosive wear can be one of the reason for poor performance of the existing models. One of the type of corrosive wear is oxidative wear in which material's surface react with oxygen. Qin et al. (2018) concluded that main wear mechanisms for corrosion resistant alloys (CRA) were adhesive, abrasive and oxidative wear. The downhole casing wear mechanism is complex. It is difficult to determine the effect of each mechanism and predict their occurrence. Furthermore, these mechanism can occur in combination. Also there can be instances where some are active and other times all may have an effect. A correction factor is utilized in the model as presented in equation (6) which is based on experimental test data from carbon steel material. Today, the only way to account these effects for CRA, is to change the wear factor in the fundamental equation [2] [3].

2.4 Factors Affecting Casing Wear

It is vital to discuss the parameters and uncertainties that effects the material affinity to casing wear. Some of the key elements are mention below:

2.4.1 Torque & Drag Models

The soft and stiff string models are used to simulate side forces and both models have different applications. For instance the wells which have low dogleg, the difference between these models is negligible. However, the difference is significant for high dogleg wells and the stiffness of pipe should be added. The models on the market are good for steel casings but need to be more detailed for CRA material which is much more susceptible for wear.

2.4.2 Dogleg Severity

Side force is greatly influence by curves in the well paths. Aggressive doglegs often increase the side force significantly. Shallow DLS have more impact than the deeper ones, because of higher string weights.

2.4.3 Mud Type

The mud type has an indirect impact on casing wear and effect the friction in wellbore. Therefore, one of the key input in T&D models is the friction factor (FF). Oil based mud (OBM) generates less friction between drill pipe and casing as compared to water based mud (WBM). However, the friction factor contains many elements and is therefore uncertain. Lubricants can be added in mud to decrease friction.

2.4.4 Tool Joint OD

Tool joint OD is related to the sliding distance and contact pressure. If the tool joint OD is increased then sliding distance will increase which will effect wear volume. However, the contact pressure decreases with increase in tool joint OD due to larger contact area. Therefore, OD of drill pipe has a tradeoff situation for casing wear.

2.4.5 Rate of Penetration (ROP) & RPM

Both ROP and RPM are related to the sliding contact exposure along casing wall. Equation (2) clearly indicates that the casing will experience less wear by minimizing the rotating hours. Therefore, the RPM should be as low as possible and the ROP should be high. When the ROP is low then the RPM will have significant effect on wear due to increased exposure in time and the number of rotations.

2.4.6 Weight on Bit (WOB)

Weight on bit (WOB) affects the side force. If the WOB is increases then neutral point will shift upward which will leave less part of drill string in tension. A reduction in tension will results in more contact force with the casing wall especially on low side of wellbore. However, the variation of WOB has smaller effect on overall results.

2.5 Recommended Drill pipe and Casing Size Configuration

The wells from Norwegian continental shelf (NCS) with different DLS were investigated for casing wear by varying drill pipe size to suggest optimal parameters and tubing & casing size ratio. Table -2.1 shows the results obtained from casing wear simulation:

WELL	DLS deg/30m	TUBING SIZE (in)	WOB/RPM klb	WEAR % WITH 3 ½" DP	WEAR % WITH 2 7/8" DP	WEAR % WITH 2 3/8" DP
A	4.5	7	15 / 100	3.0	2.20	1.30
D	4.0	7	15 / 100	2.64	1.90	1.20
G	3.0	7	15 / 100	2.32	1.65	1.15

Table – 2.1: Casing wear simulation results

It is evident from the above mentioned results that if drill pipe size is decreased then the casing wear will also reduce. Therefore, to minimize casing wear it is recommended to use 2 3/8" drill pipes in 7" tubing. However, other operational challenges should be considered for instance; buckling of slim drill pipes, tensile strength, torque and hydraulics limitations.

3 Research and Simulation for Side Forces

As said in section 2.4.1 the side force acting between tool joint and casing is one of the key parameter for accurate prediction of casing wear and is important where doglegs are high. In the NCS, TTRD operation is a common technique used to cost effectively drain small reservoir targets. However, reaching new targets from old wells often involves high doglegs which can be seen from some of the reference wells mention in the appendix. The high doglegs and TTRD operations can cause severe tubing wear issues. Therefore, it is essential to include all details of the operations when modeling to predict wear accurately and subsequently to know that the well has adequate integrity after operation is over. Following the list of parameters influencing wear mentioned in section 2.4, number of wells were investigated to map the span of side force experienced.

A large number of TTRD wells in the NCS were investigated to ensure a good cover of all effects that can influence the side forces. Criteria's used in selection was:

a) Deep and shallow reservoirs
b) Long TTRD section
c) High dog legs in TTRD section

Eight wells were selected based on these criteria's. An imaginary well was added in simulation after discussion with experienced professionals to ensure a realistic but at the same time worst case situation with the highest possible side forces.

3.1 Inputs

Landmark's WellPlan was used to model the well side forces for all the selected wells. All the required data used for simulation such as well trajectory, bottom hole assembly (BHA), fluid properties and flow rates has been obtained from the operational reports of the NCS wells. The operational parameters are given in Table -3.1:

WELL	TOP OF RESERVOIR MD (m)	TOTAL DEPTH MD (m)	DLS deg/30m	TTRD LENGTH (m)	TUBING SIZE (in)	FRICTION FACTOR CH / OH	WOB klb	FLOW RATE gpm
A	5548	5898	4.5	350	7	0.25 / 0.30	15	180 – 200
B	3842	5537	3.5	1694	7	0.25 / 0.30	15	180 – 200
C	1733	2851	5.0	1118	7	0.25 / 0.30	15	180 – 200
D	3335	4469	4.0	1134	7	0.25 / 0.30	15	180 – 200
E	2637	3995	5.0	1358	7	0.25 / 0.30	15	180 – 200
F	3069	4669	3.5	1560	7	0.25 / 0.30	15	180 – 200
G	2998	3722	3.0	724	7	0.25 / 0.30	15	180 – 200
H	2223	4069	4.0	1846	7	0.25 / 0.30	15	180 – 200
TEST	4098	5440	5.0	1342	7	0.25 / 0.30	15	180 – 200

Table - 3.1: Inputs for side force simulation

Fig 3.1 shows the directional profile of imaginary well.

Fig 3.1: Well trajectory for imaginary well

Figure 3.2 shows the 3-D view of the well -A from Norwegian continental shelf (NCS).

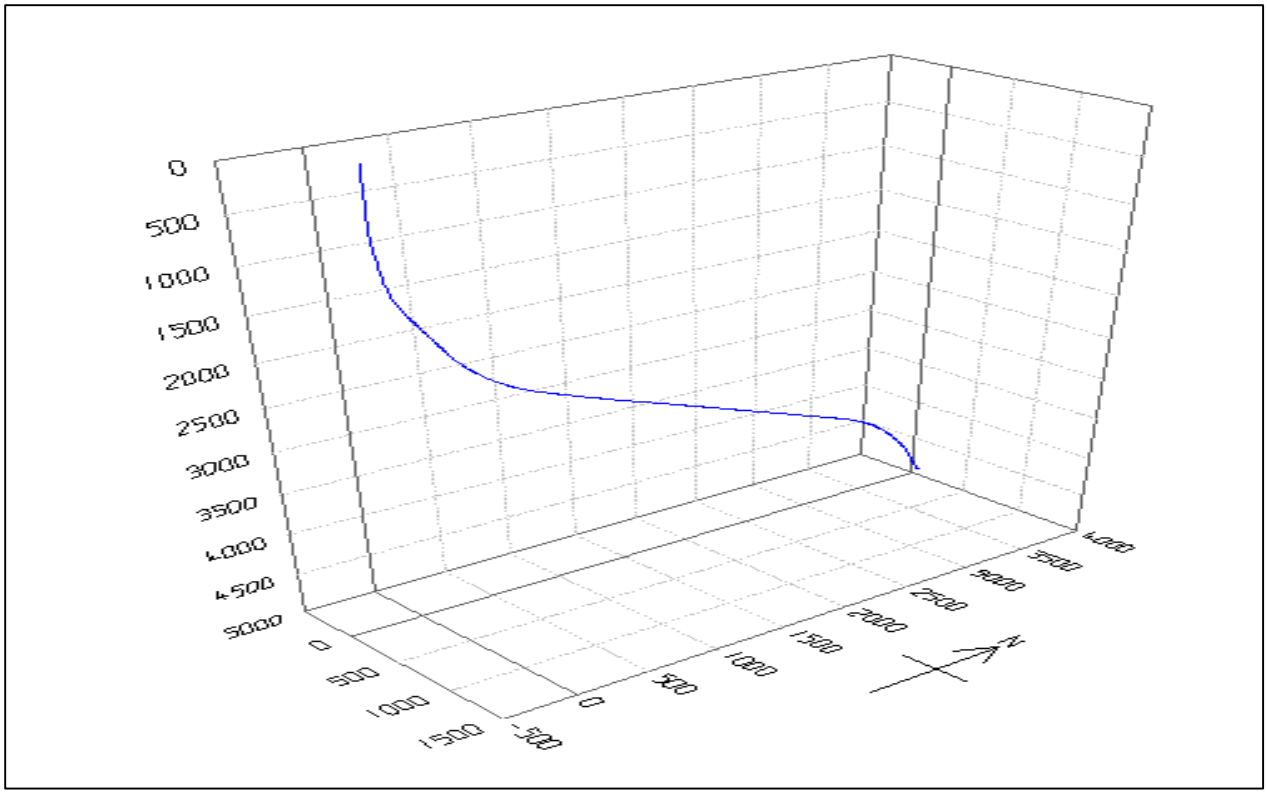

Fig 3.2: 3-D view of the Well A

3.2 Results

The Results for imaginary well and one well from NCS will be presented below, however for other wells please refer to appendix -9.1.Fig 3.3 depicts the resulting side force which is indicating the maximum side force of 6000 lbf/length at approximately 2500m TVD. This shallow dogleg is sometimes be found in wells with prior sidetrack or slot recovery.

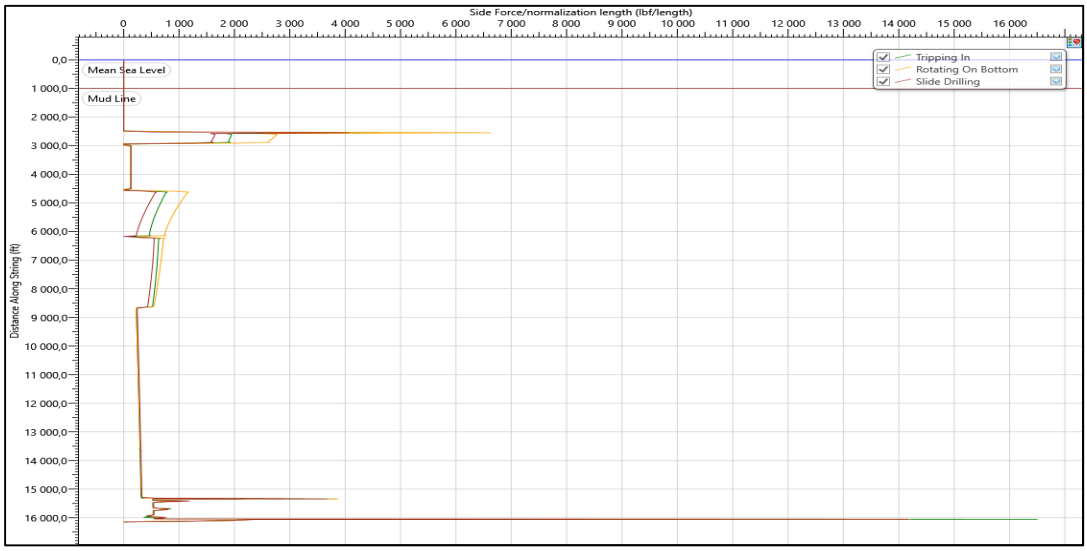

Fig 3.3: Modelled side force plot for test well

Figure 3.4 illustrates the result of side force for NCS well A.

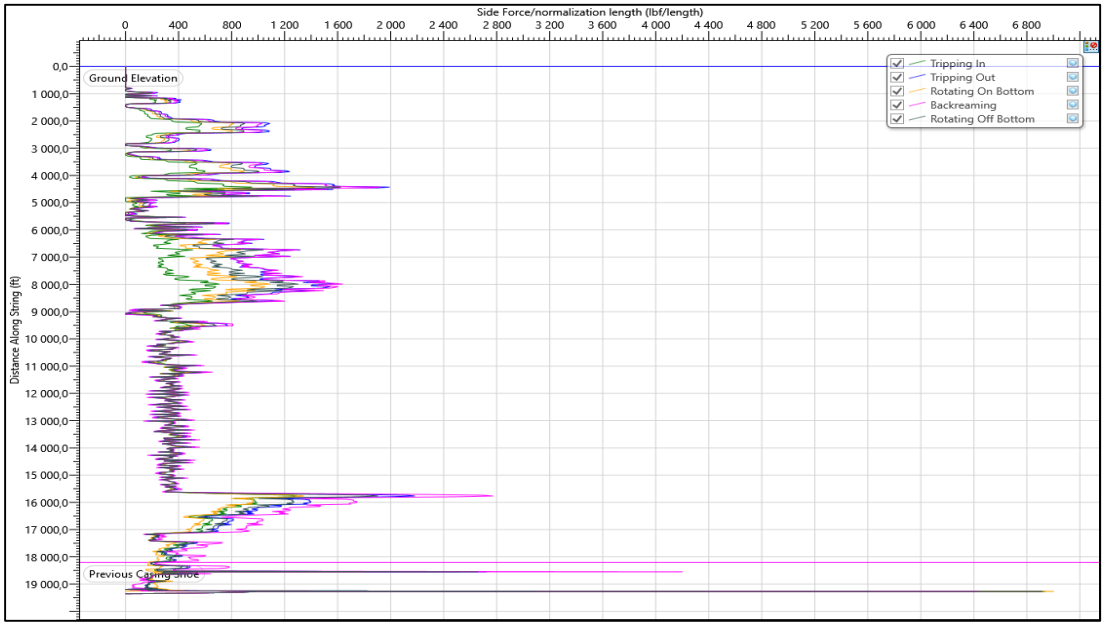

Fig 3.4: Modelled side force plot for Well A

The summarized results for side forces are given in below Table - 3.2. Apart from the imaginary well, the side force is in the range from 500 to 2000 lbf/length which is typically for all TTRD wells investigated.

WELL	LOW SIDE FORCE lbf/length	MAX SIDE FORCE lbf/length
A	200	2300
B	350	1320
C	150	900
D	300	1830
E	200	1200
F	160	2000
G	200	2050
H	150	2200
TEST	250	6500

Table – 3.2: Simulated side forces

Based on these simulated side forces, a test matrix was discussed with industry professionals and presented in Table 4.3:

TEST #	SIDE FORCE lbf/length	13CR80 RPM	13CRS110 RPM
1	250	155	155
2	500	30 / 155	30 / 155
3	1500	155	155
4	3000	30 / 155	30 / 155
5	6000	155	155

Table – 4.3: Designed test matrix

4 Laboratory Wear Testing

The wear testing apparatus was built to meet the requirements and guidelines in API CW7 (2012). The test rig used a real 3 ½" drill pipe tool joint and accommodates a section of 7" tubing / casing of the 13Cr80 and the 13CrS110 materials.

4.1 Experimental Setup

The apparatus for wear testing follows the relevant API standard and the procedures are the one used in DEA-42 for comparison. Figure 4.1 shows the principle apparatus while figure 4.2 depicts actual test rig. During the testing, there is a continuous measurement of the remaining wall thickness of the casing specimen. It was a time based measurement while the apparatus run at the chosen operational parameters. The key operational parameters are RPM, side force, drilling fluid and ultrasonic sensor [*Andreas Teigland 2021*]:

4.1.1 RPM

The tool joint was welded to a flange and motor was used to rotate the tool joint with constant RPM. The RPM was controlled and logged by a computer program. API recommends testing to be perform with155 RPM, which therefore used in all performed tests.

4.1.2 Side Force

The side force is applied by a pneumatic system through compressed air. The side load was controlled by a computer program and was measured from two load cells. One in the vertical and other in the horizontal direction to make sure the applied force was constant. API CW7 suggest a side force of 3000 lb/ft. However actual tests were performed at different side forces to simulate realistic conditions as experienced in TTRD wells mentioned in table 3.2. The reason for using actual side forces over a range was to investigate the wear characteristics depending on contact force and to find CPT if it exist for the test materials.

4.1.3 Drilling Fluid

The water based (KCL Polymer) mud was pumped through nozzles to the contact point between casing and the tool joint in a closed loop system. The temperature was controlled by a cooling system. There was no sand content considered in mud and testing due to the possible erosion of mud pump.

4.1.4 Thickness Measurement

The thickness of the casing was measured continuously during testing by an acoustic sensor installed on the side of casing specimen. In order to make sure the contact between sensor and casing specimen throughout the test, the acoustic sensor was coupled with silicone grease.

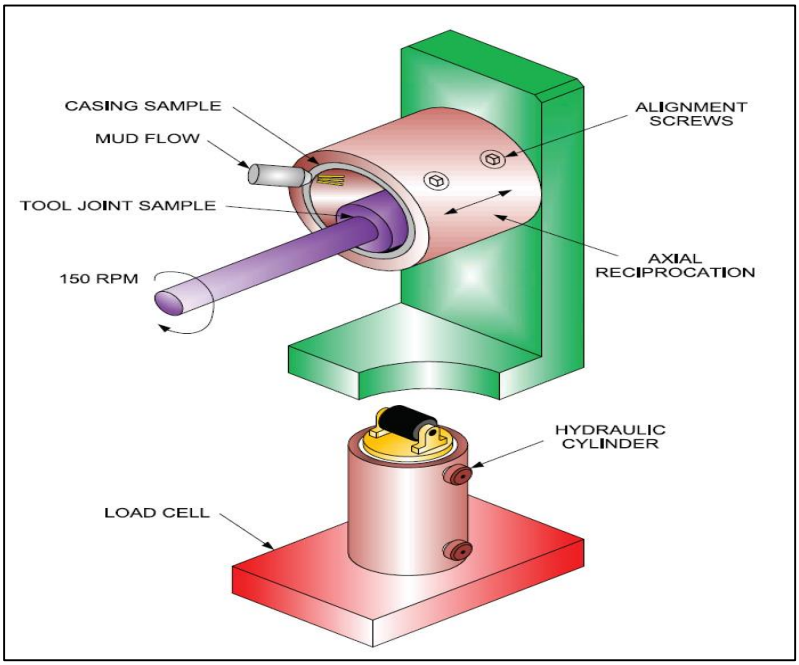

Fig 4.1: API test apparatus [8]

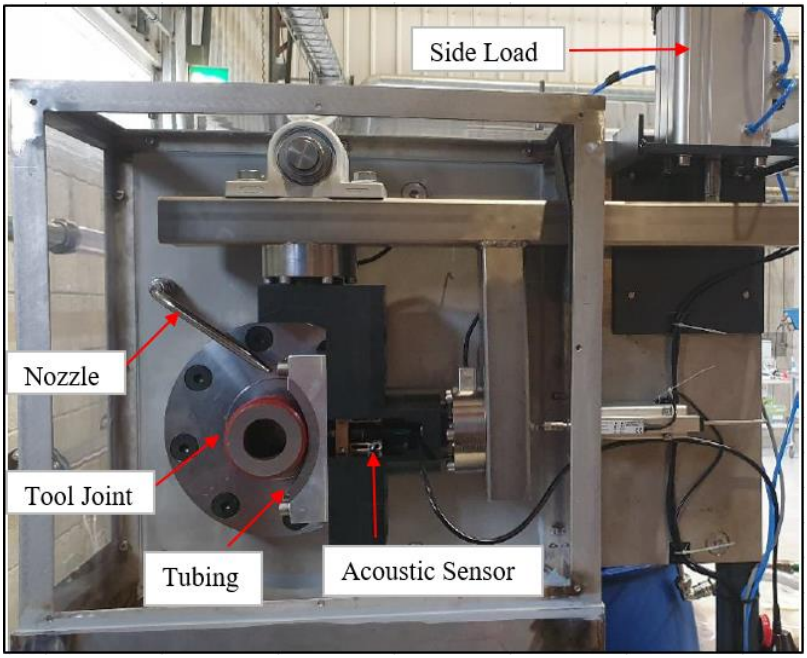

Fig 4.2: Actual test rig

4.2 Test Conditions

The industry standard test conditions are listed in Table 4.1;

PARAMETER	UNIT	VALUE
Side Load Per Unit Length	lbf/ft	3000
Rotational Speed	RPM	155
Casing Od	in	9 5/8
Casing Thickness	in	0.595
Casing Length	in	4.0
Tool Joint OD	in	6.25
Tool Joint Length	in	3.25
Mud Flow Rate	gpm	1.5 – 3.0
Mud Density	ppg	9.90 – 10.1
Sand Content	vol%	7.0
Marsh Funnel Viscosity	sec	50 – 60

Table 4.1: Standard test condition

The actual test conditions are summarized in below Table 4.2. There is some difference in planned and actual side forces due to the limitation of test rig. Test rig can provide maximum 4300 lb/ft and minimum 650 lb/ft side force.

PARAMETERS	UNIT	TEST -1	TEST -2	TEST -3	TEST -4	TEST -5	TEST -6	TEST -7	TEST -8
Casing Grade		13Cr80	13Cr80	13Cr80	13Cr80	13CrS110	13CrS110	13CrS110	13CrS110
Side Load	Lbf/ft	4300	3200	1550	650	650	1550	3200	4300
Rotational Speed	RPM	155	155	155	155	155	155	155	155
Casing OD	in	7	7	7	7	7	7	7	7
Casing Thickness	in	0.420	0.405	0.412	0.410	0.470	0.469	0.441	0.455
Casing Length	in	3.27	3.27	3.27	3.27	3.27	3.27	3.27	3.27
Tool Joint OD	in	3.34	3.34	3.34	3.34	3.34	3.34	3.34	3.34
Tool Joint Length	in	3.27	3.27	3.27	3.27	3.27	3.27	3.27	3.27
Mud Flow Rate	gpm	6 - 8	6 – 8	6 – 8	6 – 8	6 – 8	6 – 8	6 – 8	6 – 8
Mud Density	ppg	10.50	10.50	10.50	10.50	10.50	10.50	10.50	10.50
Sand Control	vol%	0	0	0	0	0	0	0	0
Marsh Funnel Viscosity	sec	43	43	43	43	43	43	43	43

Table 4.2: Actual test conditions

5 Results and Discussion

5.1 Test -1: 13Cr80 with Side Force = 4300 lb/ft

Test -1 was performed on 13Cr80 material with a side force of 4300 lb/ft. The other test conditions and parameters are listed in Table 3.2. Figure 5.1 shows the work function plotted against wear volume for the data obtained during the test. The measured data was curve fitted which is shown as the estimated curve in the plot. The non-linear relationship between the work function and the wear volume as predicted by equation (3) is not seen in the plot. Rather, a linear relationship is found between these parameters. This indicates no CPT at 4300 lb/ft side force, as depicted in figure 5.2.

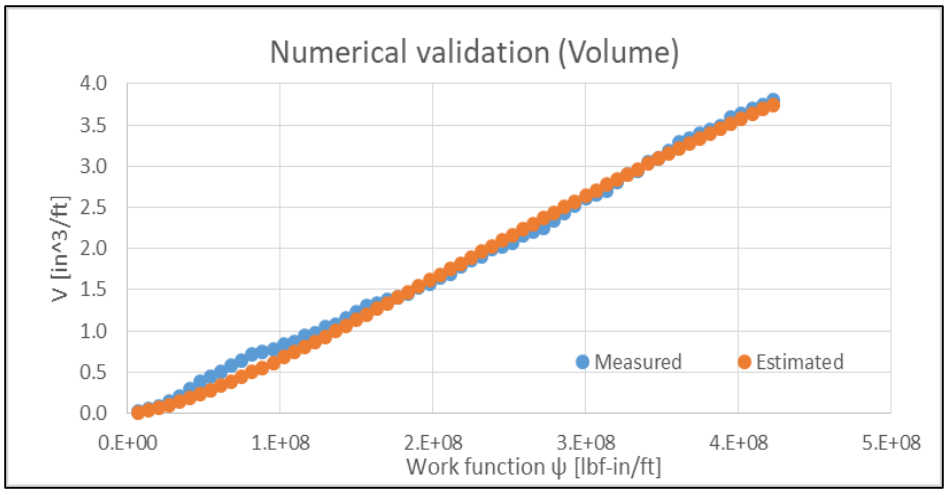

Fig 5.1: Wear volume vs Work function for 13Cr80 at 4300 lb/ft

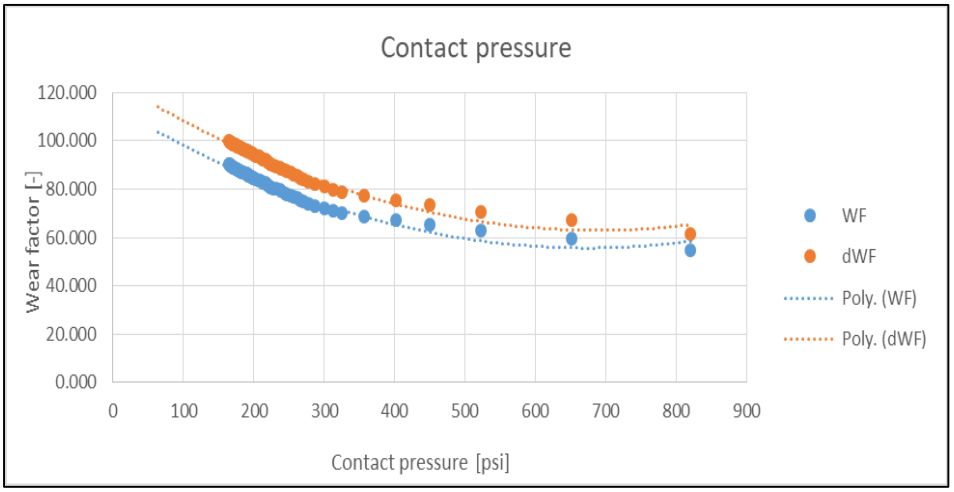

Fig 5.2: Wear Factor vs Contact Pressure for 13Cr80 at 4300 lb/ft

Figure 5.3 shows the measured wear percentage as a function of time. The casing sample was worn to 50% of the original wall thickness. It is important to note that only one hour was required to achieve this degree of wear. This indicates that 13Cr80 is prone to high wear rates at 4300 lb/ft side force. This side force was also higher than the modelled side force experienced in any of the NCS offset TTRD wells.

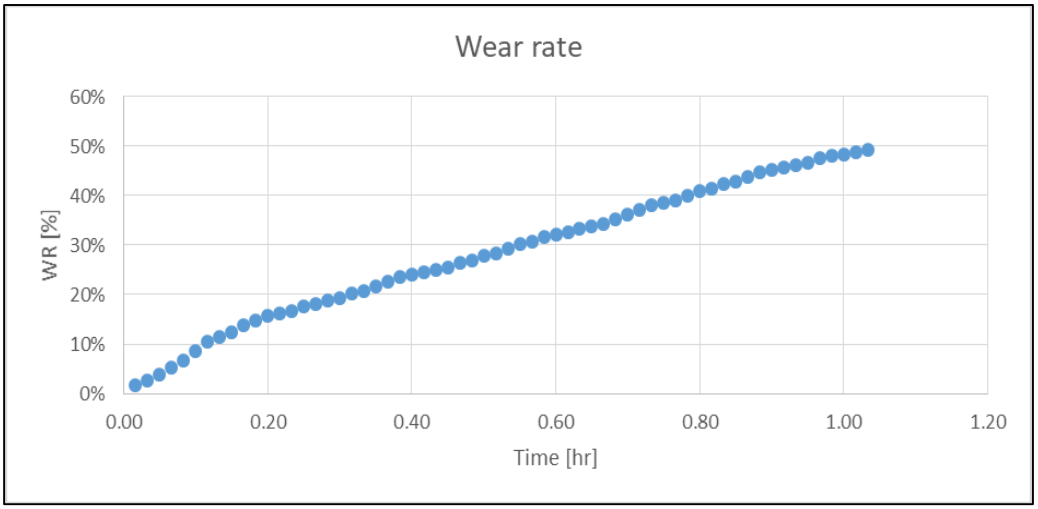

Fig 5.3: Wear rate vs Time for 13Cr80 at 4300 lb/ft

Figure 5.4 depicts wear factor against test time. There are fluctuations in the wear factor during initial intervals, but it stabilizes and becomes constant. The wear factor converges to 90 E-10 psi^{-1} which is significantly larger than commonly used wear factors. The trend of the test coincides with experiment performed by (Andreas Teigland 2021). The only difference was the applied side force.

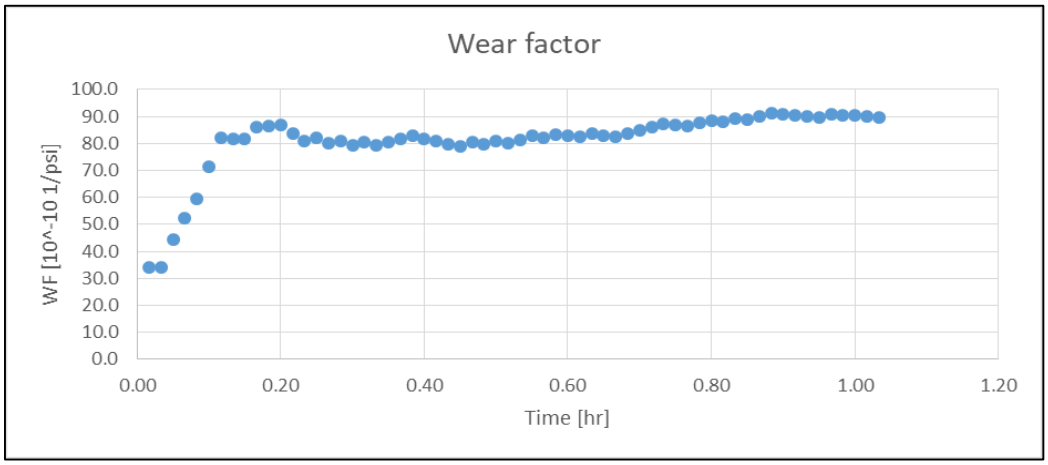

Fig 5.4: Wear Factor vs Time for 13Cr80 at 4300 lb/ft

5.2 Test -2: 13Cr80 with Side Force = 3200 lb/ft

Test -2 was performed on 13Cr80 material with a side force of 3200 lb/ft. Figure 5.5 shows the work function plotted against wear volume for measured value. The data was curve fitted which is shown as the estimated curve in the plot. Similar to previous Test -1, a linear relationship is found between work function and wear volume, which indicates no CPT at 3200 lb/ft side force as depicted in figure 5.6.

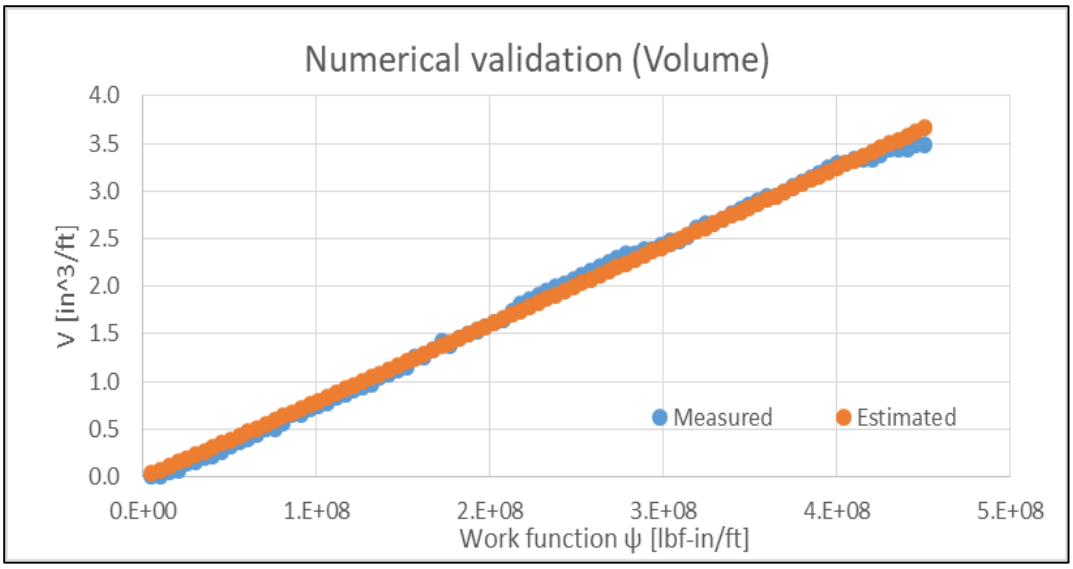

Fig 5.5: Wear volume vs Work function for 13Cr80 at 3200 lb/ft

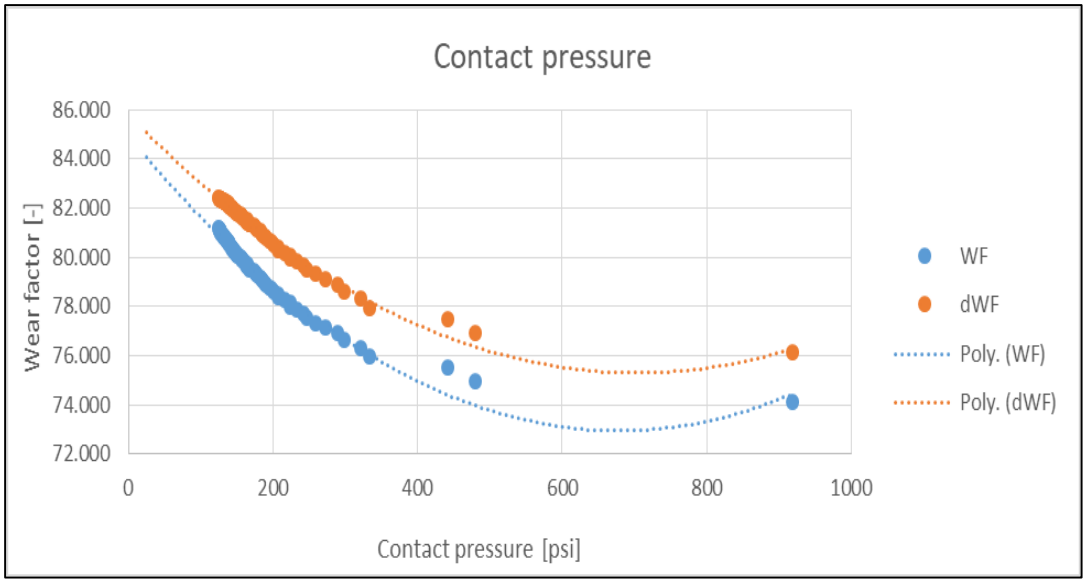

Fig 5.6: Wear Factor vs Contact Pressure for 13Cr80 at 3200 lb/ft

Figure 5.7 shows the measured wear percentage as a function of time. The casing sample was worn to ~50% of original wall thickness in 1.5 hours. The rate of wear is similar to Test -1 indicating a rapid wear mechanism for 13Cr80 at 3200 lb/ft side force.

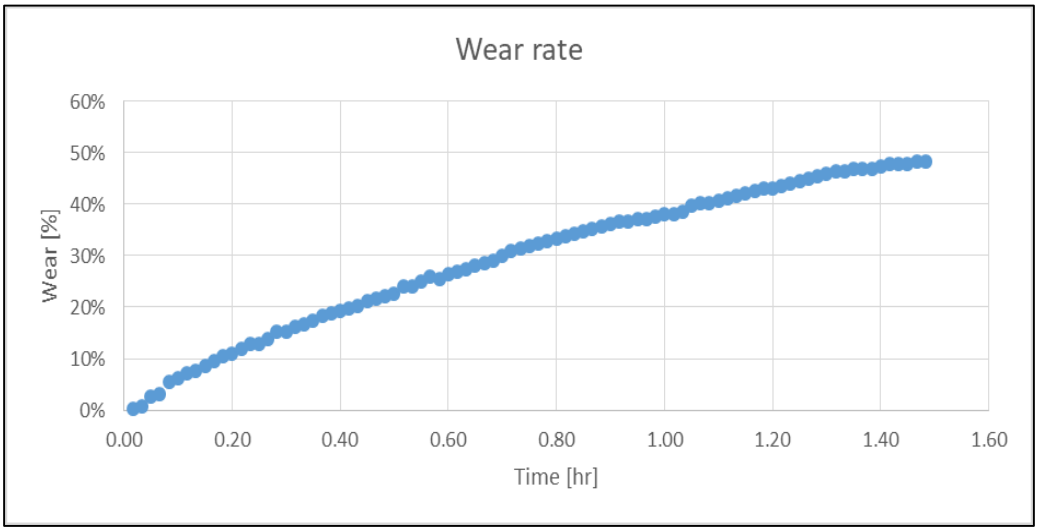

Fig 5.7: Wear rate vs Time for 13Cr80 at 3200 lb/ft

Figure 5.8 depicts the wear factor as a function of time for test -2. The trend is similar to Test -1 with initial fluctuations in the wear factor, but it stabilizes and becomes constant. The WF converges to 80 E-10 psi^{-1}. This indicates that chrome casing is subject to extremely rapid wear at 3200 lb/ft side force. The trend of the test coincides with experiment performed by (Andreas Teigland 2021) with only slight difference is in applied side force.

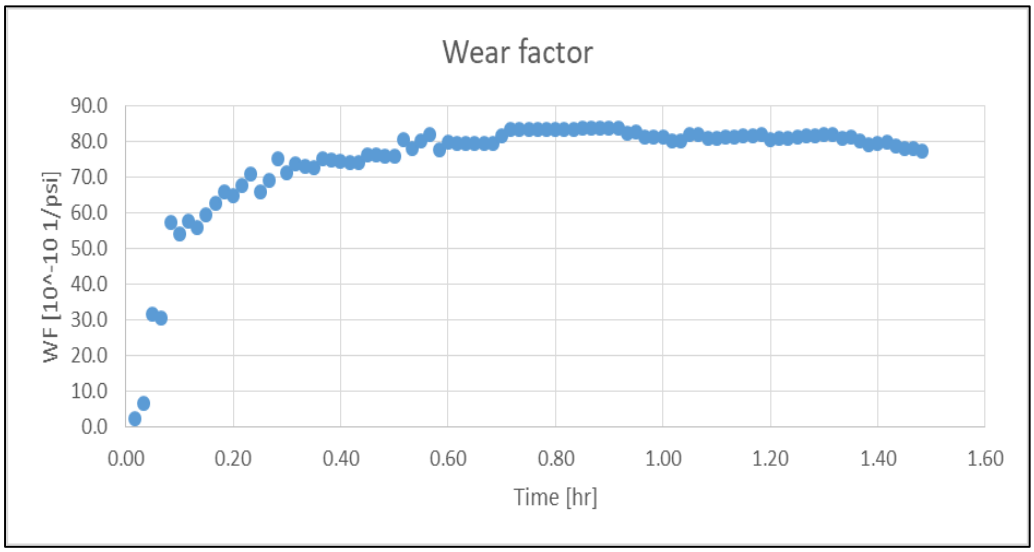

Fig 5.8: Wear Factor vs Time for 13Cr80 at 3200 lb/ft

5.3 Test -3: 13Cr80 with Side Force = 1550 lb/ft

Test -3 was performed on 13Cr80 material with a side force of 1550 lb/ft. Figure 5.9 shows the work function plotted against wear volume for the measured value. The data was curve fitted which is represented as estimated curve in the plot. Contrary to the previous two tests, a non-linear relationship is found between work function and wear volume. This is in accordance with equation (3). It indicates an existence of CPT. Figure 5.10 shows the contact pressure plotted as a function of WF. There is bending in both WF and dWF so the trend line in the plot may indicate a wrong value of CPT.

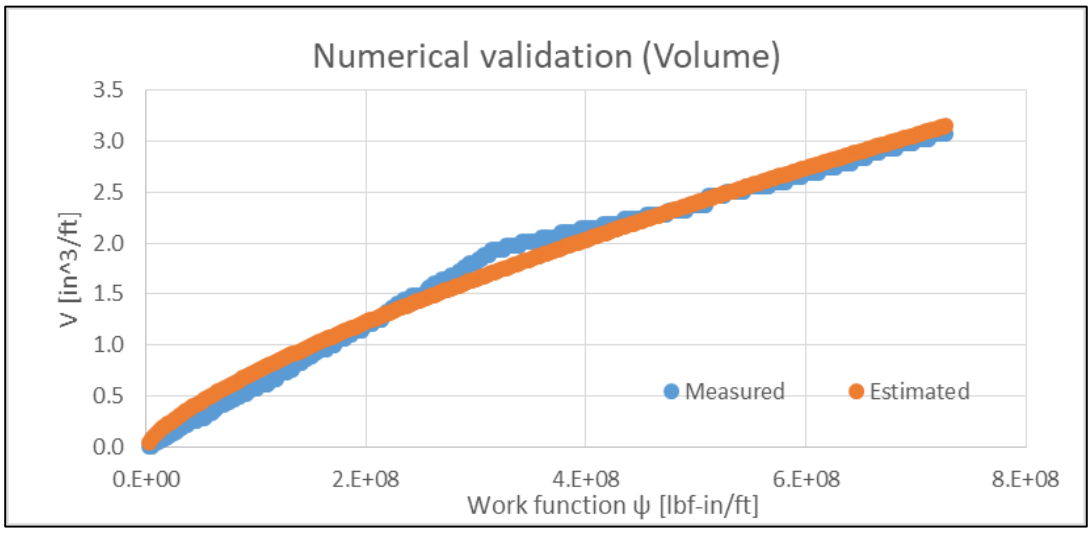

Fig 5.9: Wear volume vs Work function for 13Cr80 at 1550 lb/ft

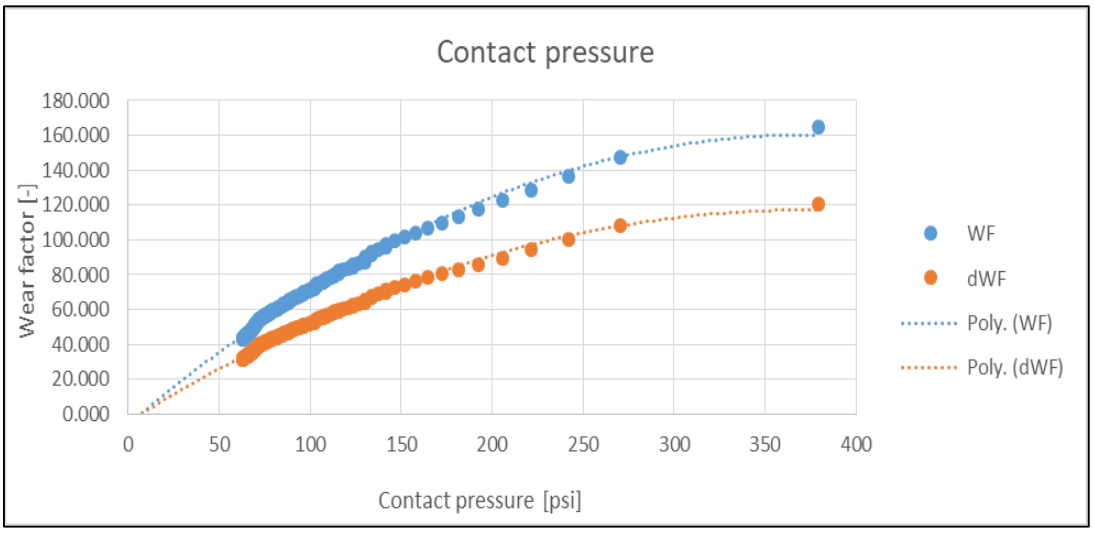

Fig 5.10: Wear Factor vs Contact Pressure for 13Cr80 at 1550 lb/ft

Figure 5.11 shows the measured wear percentage as a function of time. The casing sample was worn to ~45% of original wall thickness in almost 5 hours. The rate of wear is less than previous two tests but it is still rapid than standard steel material indicating fast wear mechanism for 13Cr80 even at 1550 lb/ft side force.

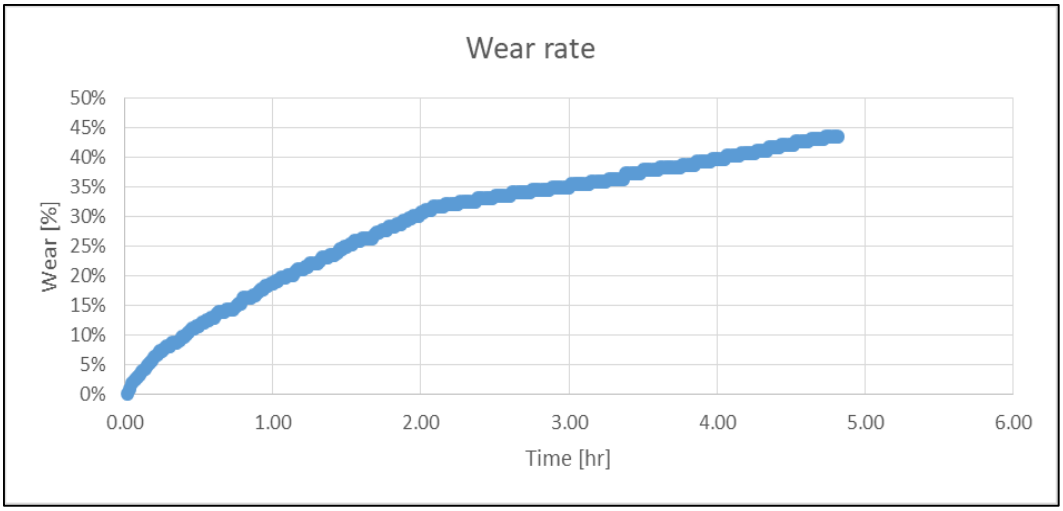

Fig 5.11: Wear rate vs Time for 13Cr80 at 1550 lb/ft

Figure 5.12 depicts wear factor against test time at 1550 lb/ft side force. The initial trend is similar to the previous two tests. After 2 hours, there is constant decline in wear factor which coincides with the wear characteristics of carbon steel material. It indicates the existence of CPT for CRA material. The same data is re-plotted in figure 5.13, starting from 2 hours of testing to show the declining trend.

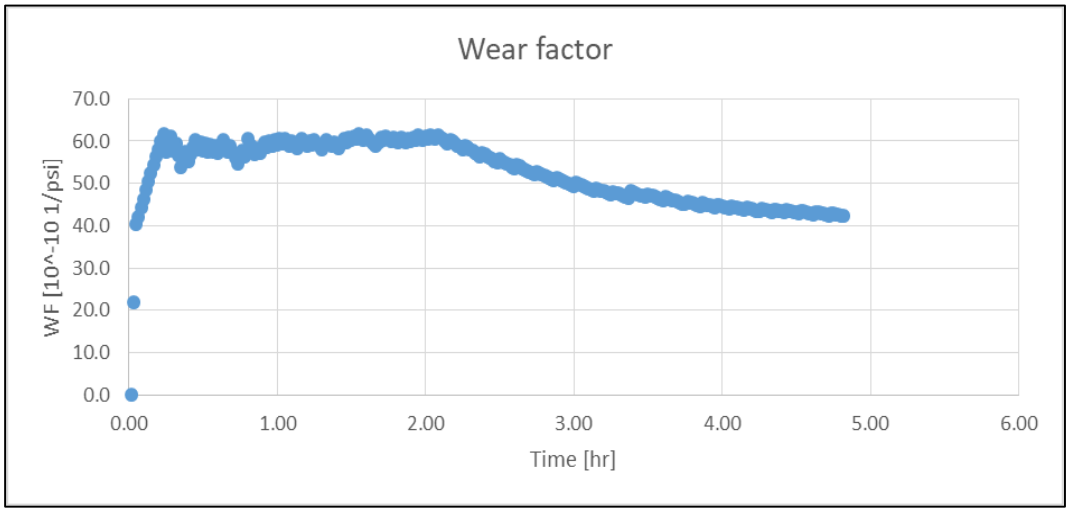

Fig 5.12: Wear Factor vs Time for 13Cr80 at 1550 lb/ft

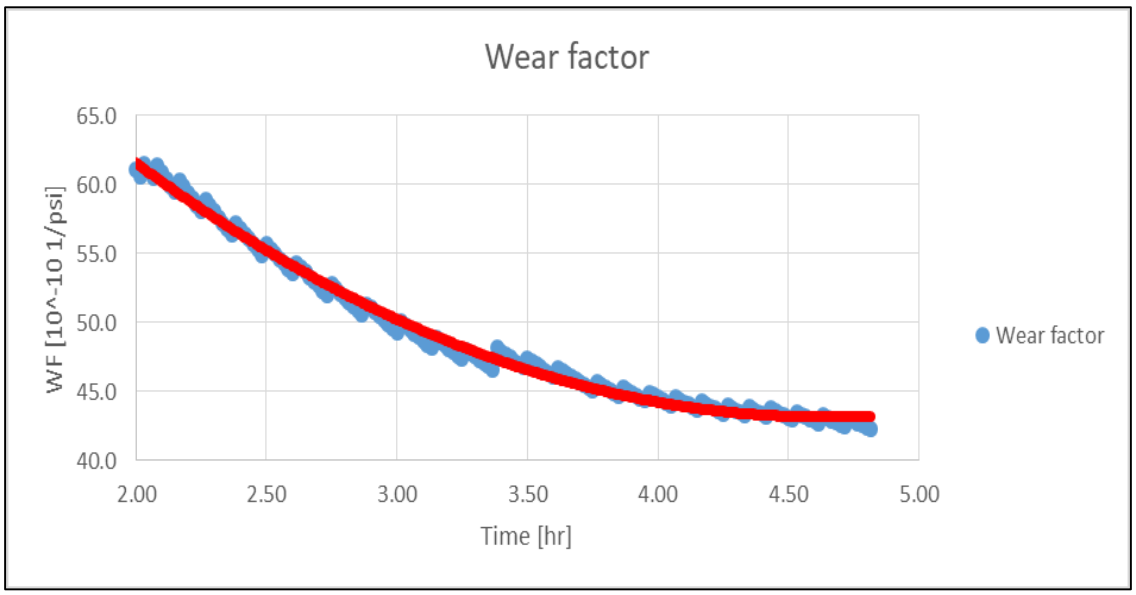

Fig 5.13: Wear Factor vs Time for 13Cr80 at 1550 lb/ft after 2 hours of test

5.4 Test -4: 13Cr80 with Side Force = 650 lb/ft

Test -4 was performed on 13Cr80 material with side force of 650 lb/ft which was the lowest side force possible from the test rig. Figure 5.14 shows the work function plotted against wear volume for the measured values. The data was curve fitted which is represented as estimated curve in the plot. Similar to Test 5, there is a non-linear relationship found between the work function and the wear volume. This is in accordance with equation (3). It indicates an existence of CPT at these test conditions. From figure 5.15, the CPT value was found to be ~50 psi. This test proves that chrome casing material has a CPT and will be exist between 1550 lb/ft and 650 lb/ft side force.

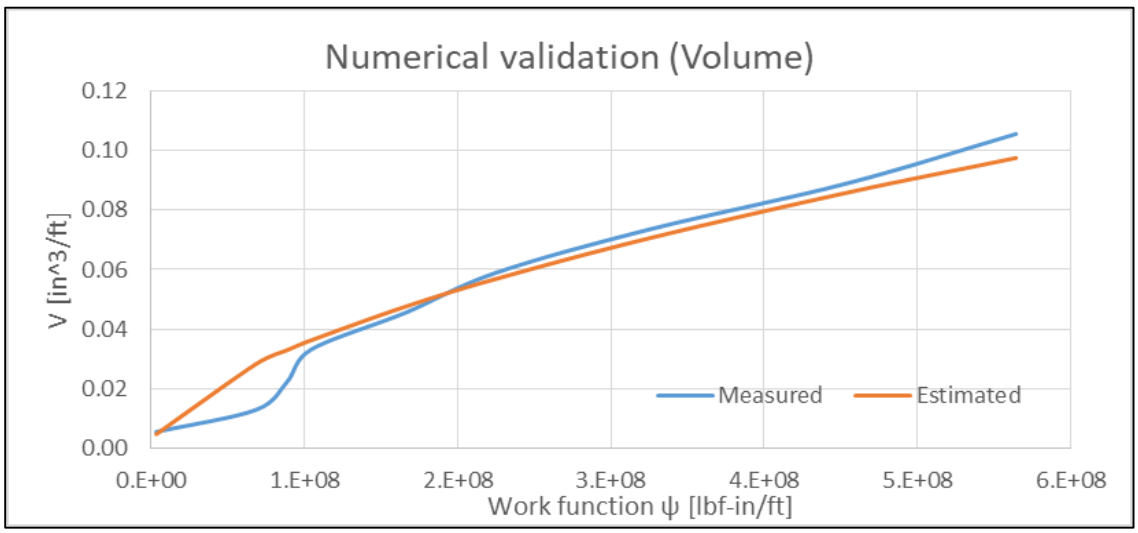

Fig 5.14: Wear volume vs Work function for 13Cr80 at 650 lb/ft

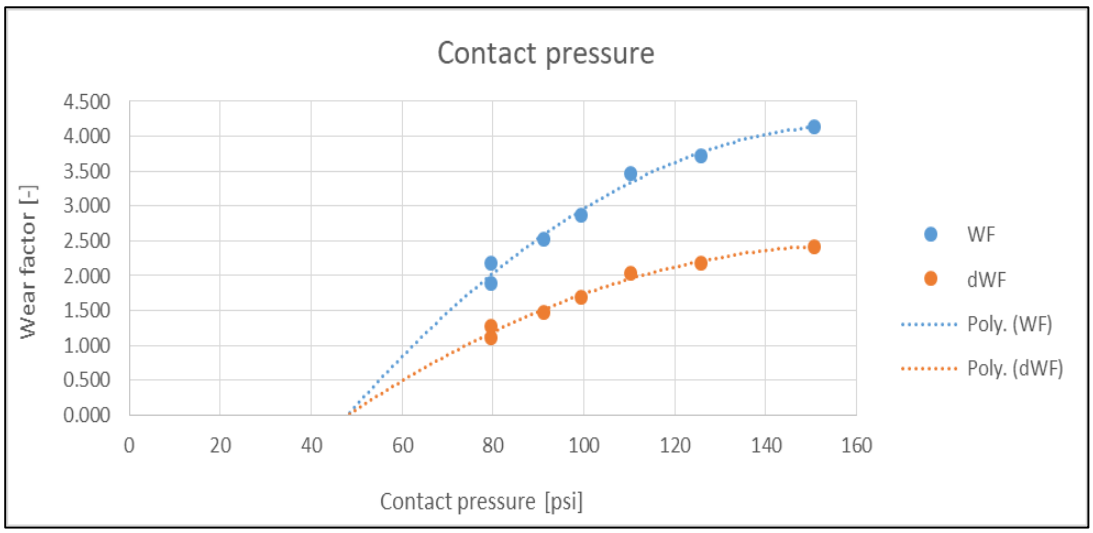

Fig 5.15: Wear Factor vs Contact Pressure for 13Cr80 at 650 lb/ft

Figure 5.16 shows the measured wear percentage as a function of time. The casing sample was worn to ~4% of original wall thickness after 4 hours. The test continued 3 hours more but no further wall loss was observed. The rate of wear is little due to low side force with a negligible rate for 13Cr80 at 650 lb/ft side force.

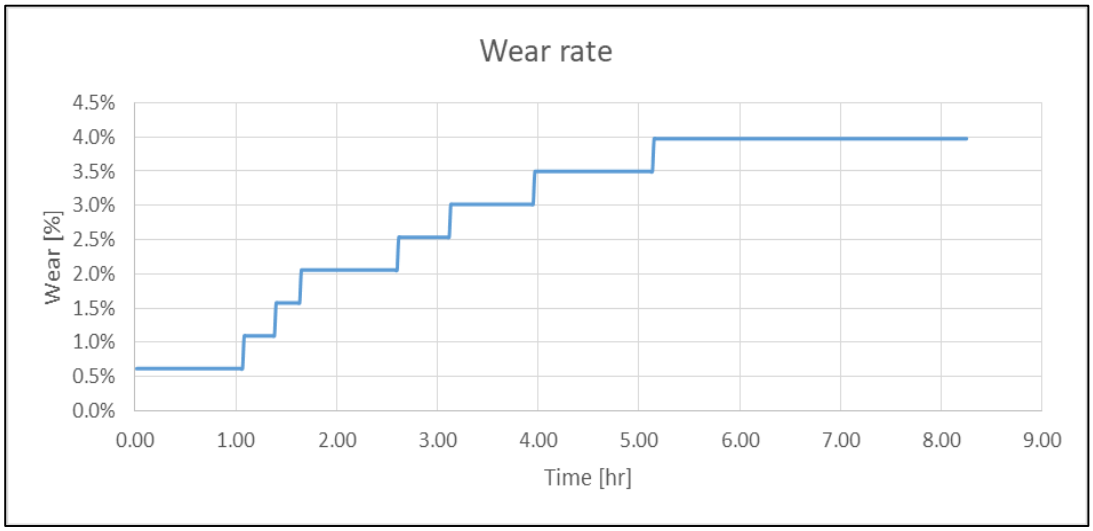

Fig 5.16: Wear rate vs Time for 13Cr80 at 650 lb/ft

Figure 5.17 depicts wear factor against test time at 650 lb/ft side force. The trend is similar to carbon steel material which strongly indicates the existence of CPT for CRA material. The wear factor stabilizes to 4.0 E-10 psi^{-1}. This indicates that chrome casing is subject to less wear at these test conditions.

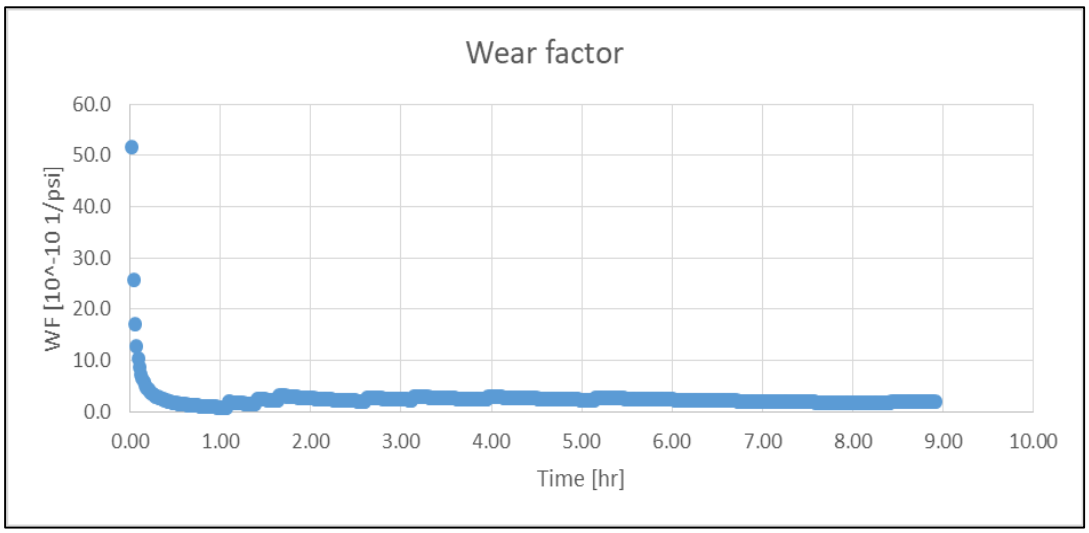

Fig 5.17: Wear Factor vs Time for 13Cr80 at 650 lb/ft

5.5 Test -5: 13CrS110 with Side Force = 650 lb/ft

Test -5 was performed on 13CrS110 material with the lowest side force of 650 lb/ft. Figure 5.18 shows the work function against wear volume for the measured data. The data was curve fitted and represented as estimated curve in the plot. Similar to Test 4, a non-linear relationship was found between the work function and the wear volume. This indicates an existence of CPT at 650 lb/ft side force for 13CrS110 casing as depicted in figure 5.19.

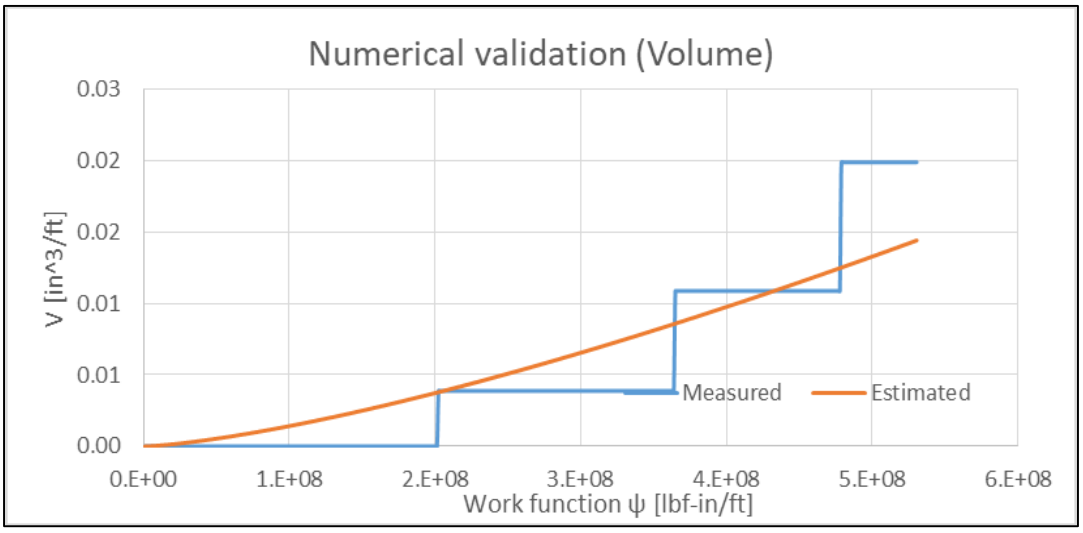

Fig 5.18: Wear volume vs Work function for 13CrS110 at 650 lb/ft

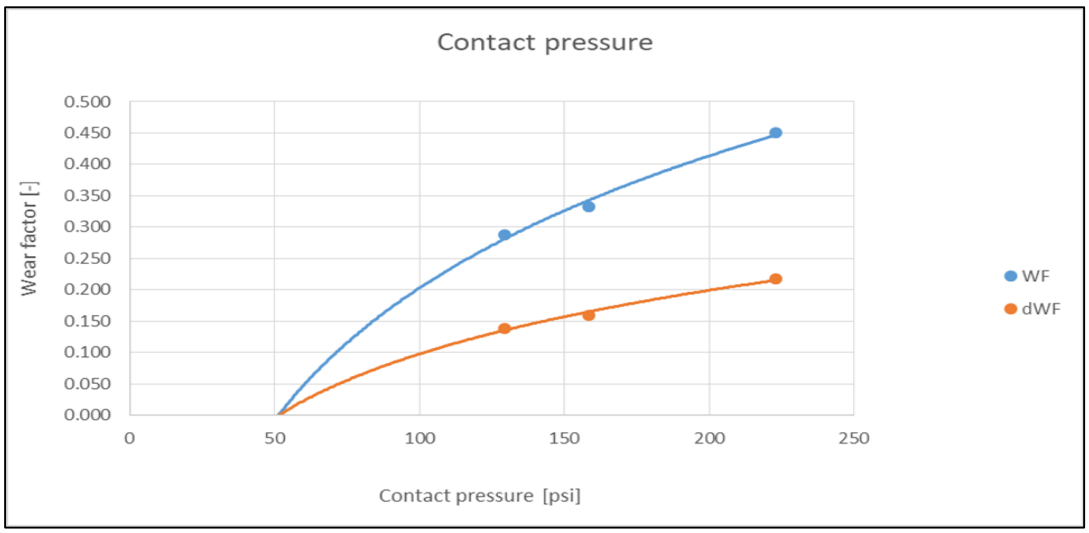

Fig 5.19: Wear Factor vs Contact Pressure for 13CrS110 at 650 lb/ft

Figure 5.20 shows the measured wear percentage as a function of time. The casing sample was worn to ~1.2% of original wall thickness in 8 hours. The rate of wear is extremely low due to low side force and hard material indicating significantly slow wear mechanism for 13CrS110 at 650 lb/ft side force.

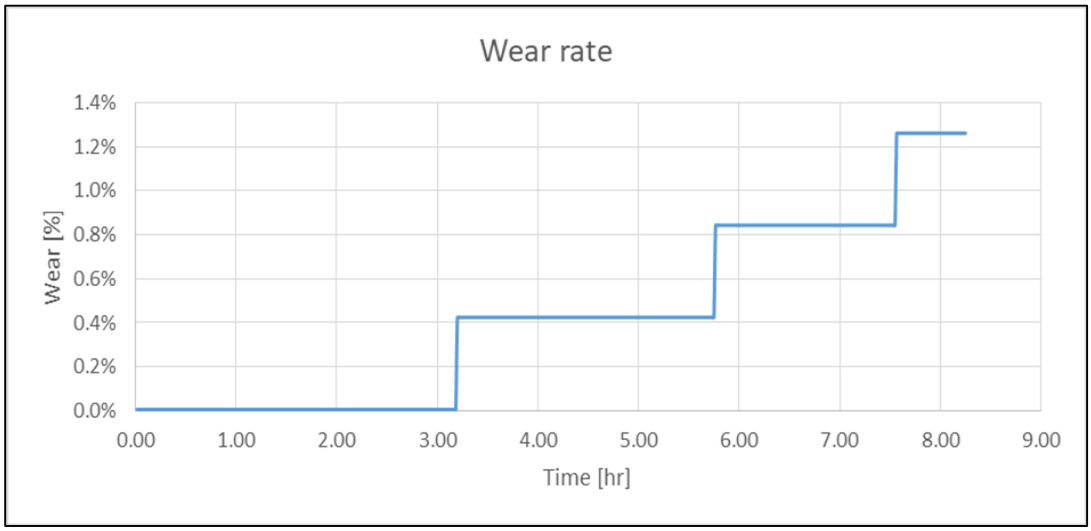

Fig 5.20: Wear rate vs Time for 13CrS110 at 650 lb/ft

Figure 5.21 depicts wear factor against test time at 650 lb/ft side force. The trend is similar to previous test -4 and coincides with carbon steel material, which further verify the existence of CPT for chrome resistant alloys (CRAs) at low side force. The wear factor is significantly low.

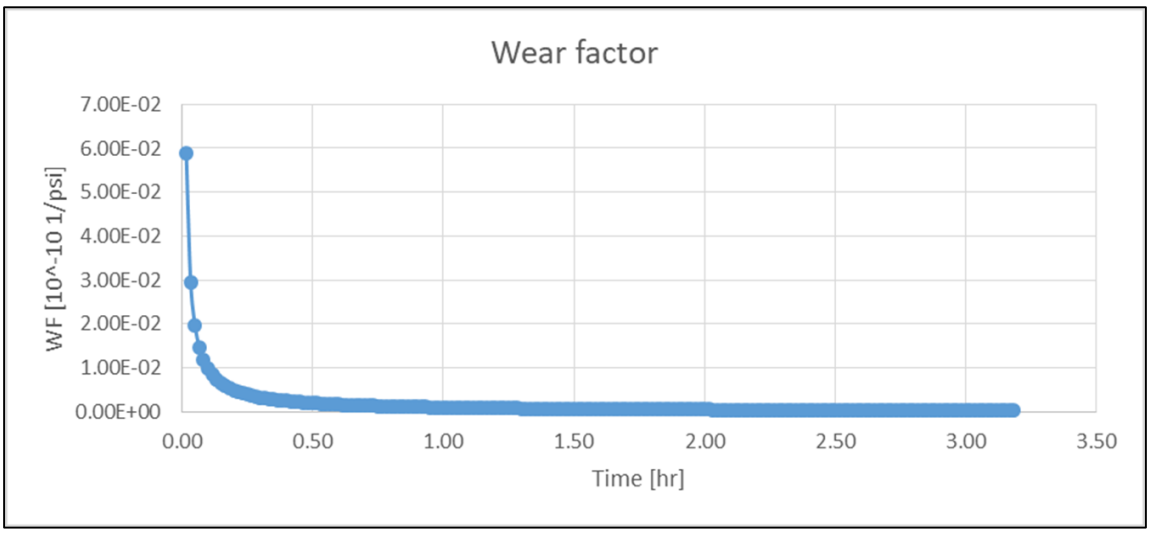

Fig 5.21: Wear Factor vs Time for 13CrS110 at 650 lb/ft

5.6 Test -6: 13CrS110 with Side Force = 1550 lb/ft

Test -6 was performed on 13CrS110 material with a side force of 1550 lb/ft. Figure 5.18 shows the work function against wear volume for the measured data. The data was curve fitted and represented as estimated curve in the plot. The trend of this test is similar to Test 3 which indicates an existence of CPT between 1550 lb/ft and 650 lb/ft side force for 13CrS110 casing as depicted in figure 5.23.

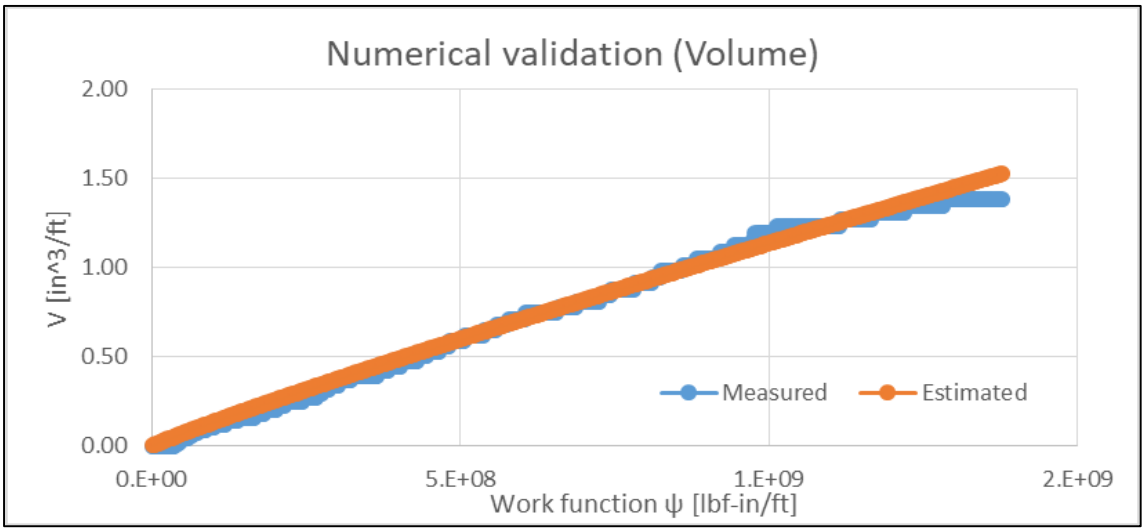

Fig 5.22: Wear volume vs Work function for 13CrS110 at 1550 lb/ft

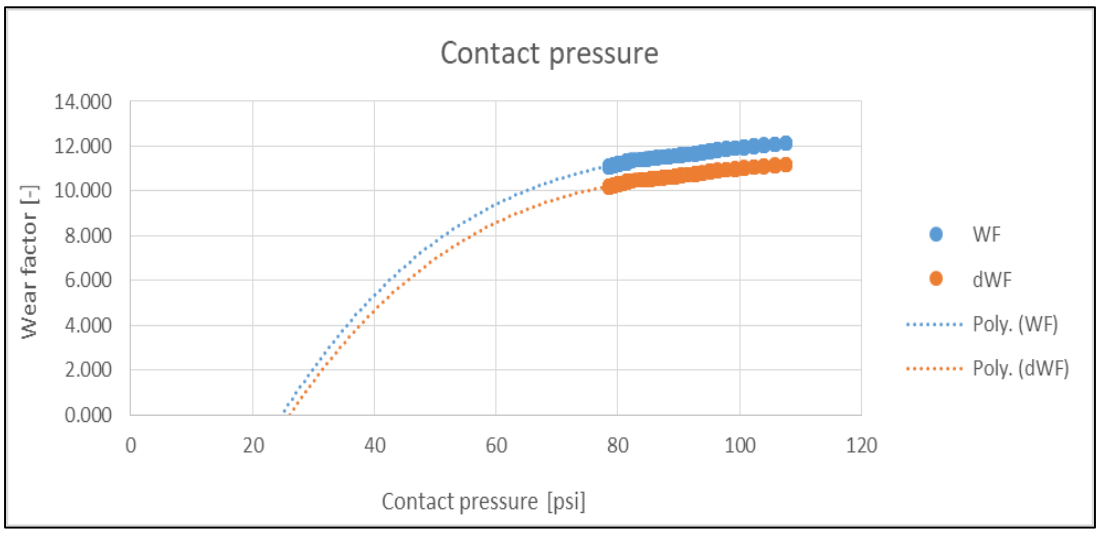

Fig 5.23: Wear Factor vs Contact Pressure for 13CrS110 at 1550 lb/ft

Figure 5.20 shows the measured wear percentage as a function of time. The casing sample was worn to ~22% of original wall thickness in 8 hours. 13Cr80 was worn down to 40% in 5 hours, while 13CrS110 was worn down 15% in the same time.

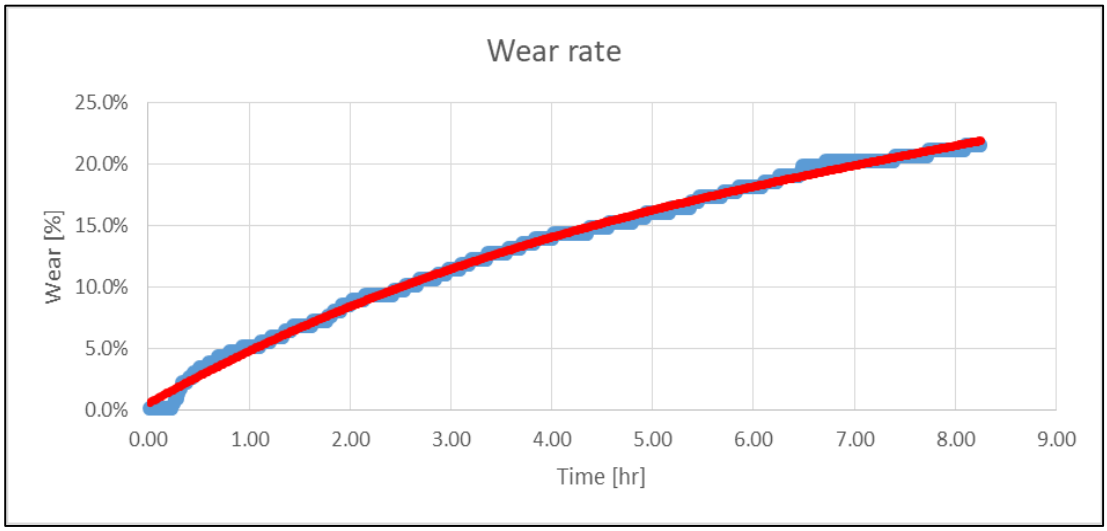

Fig 5.24: Wear rate vs Time for 13CrS110 at 1550 lb/ft

Figure 5.21 depicts wear factor against test time at 1550 lb/ft side force. There is a fluctuation at the start and later it becomes constant. It is important to note that, after 6 hours of test, the trend is declining which confirms the CPT.

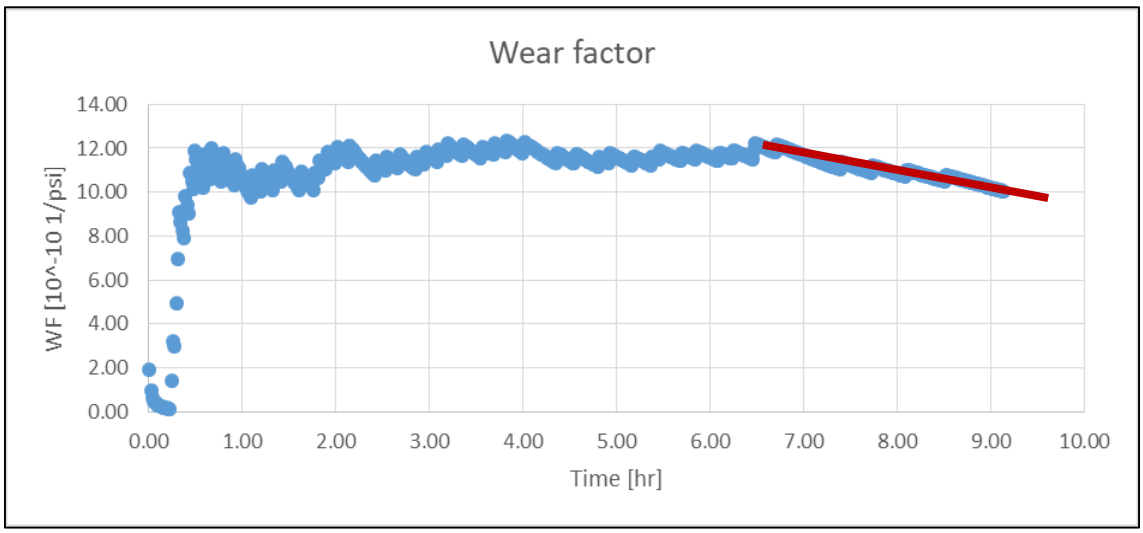

Fig 5.25: Wear Factor vs Time for 13CrS110 at 1550 lb/ft

5.7 Test -7: 13CrS110 with Side Force = 3200 lb/ft

Test -7 was performed on 13CrS110 material with a side force of 3200 lb/ft. Figure 5.26 shows the work function against wear volume for the measured data and the data was curve fitted which is shown as estimated curve in the plot. Similar to Test -1 and Test -2, a linear relationship is found between the work function and the wear volume. This indicates no CPT at 3200 lb/ft side force for 13CrS110 as depicted in figure 5.27.

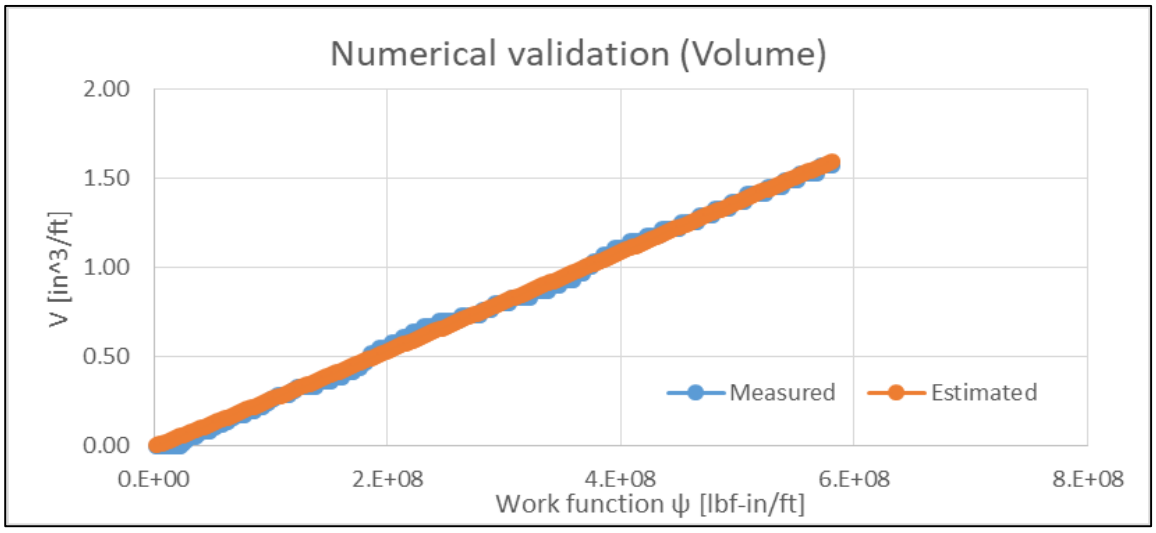

Fig 5.26: Wear volume vs Work function for 13CrS110 at 3200 lb/ft

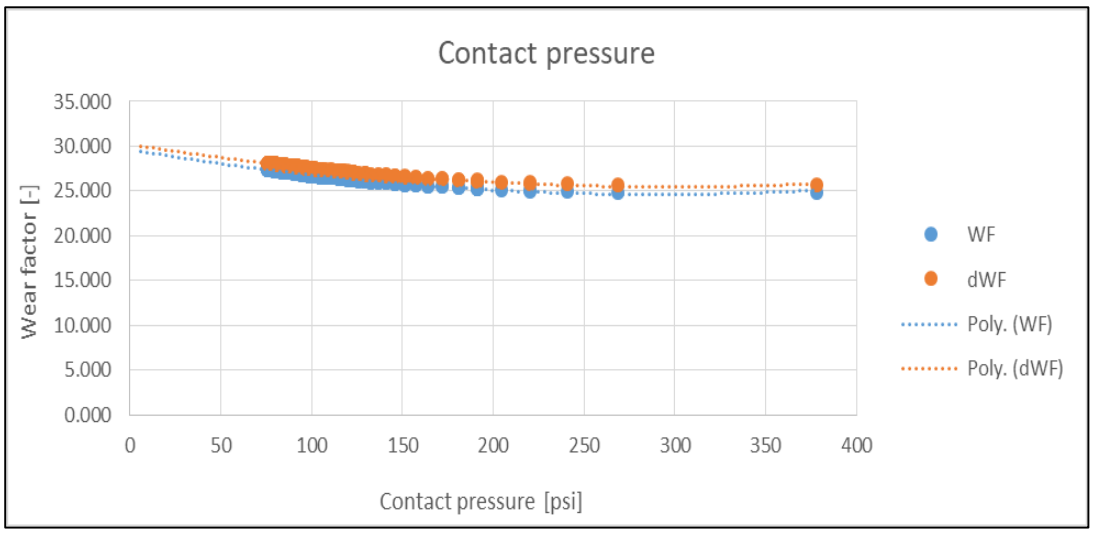

Fig 5.27: Wear Factor vs Contact Pressure for 13CrS110 at 3200 lb/ft

Figure 5.28 shows the measured wear percentage as a function of time. The casing sample was worn to ~25% of original wall thickness in 4 hours. The rate of wear is significantly less as compared to 13Cr80 material at 3200 lb/ft side force.

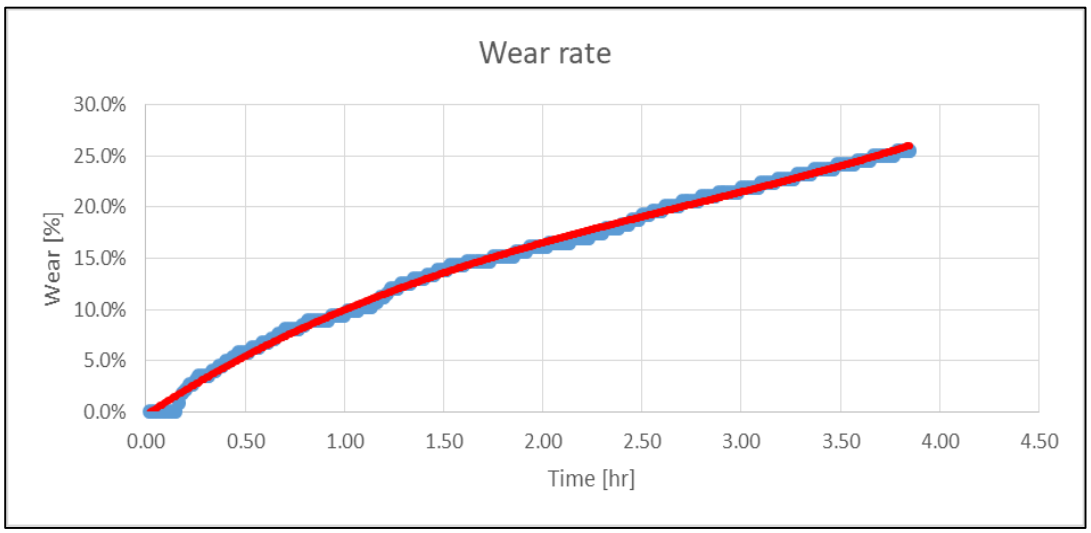

Fig 5.28: Wear rate vs Time for 13CrS110 at 3200 lb/ft

Figure 5.29 depicts wear factor against test time at 3200 lb/ft side force. The trend is similar to Test -1 and Test -2 with fluctuations in the wear factor during the initial intervals. But after 30 minutes it becomes constant and converges to 28 E-10 psi^{-1}. This value of wear factor is less than 13Cr80 material. This indicates less wear for 13CrS110 but it is still higher than regular steel material.

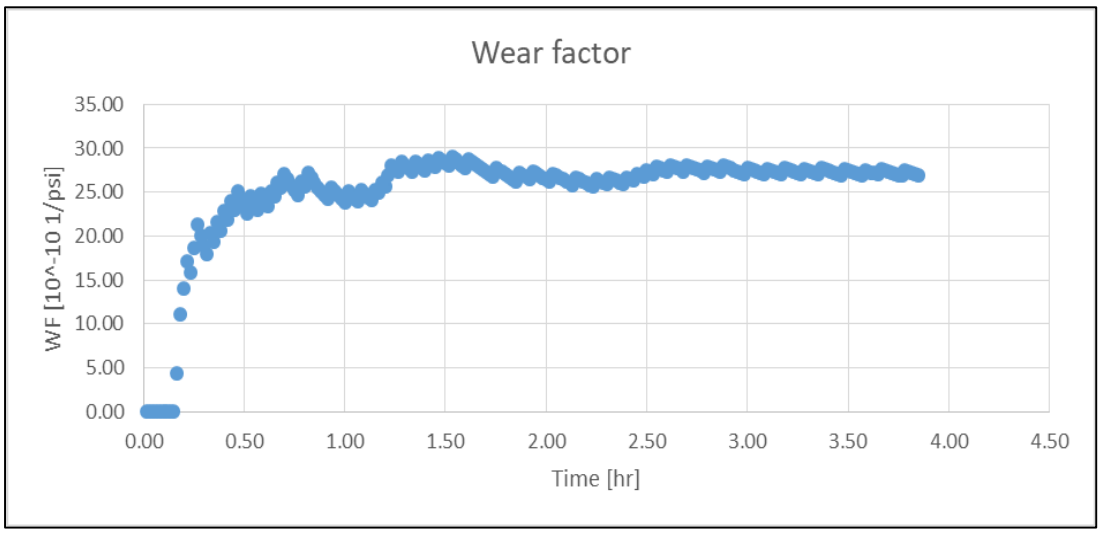

Fig 5.29: Wear Factor vs Time for 13CrS110 at 3200 lb/ft

5.8 Test -8: 13CrS110 with Side Force = 4300 lb/ft

Test -8 was performed on 13Cr80 material with a side force of 3200 lb/ft. Figure 5.30 shows the work function against the wear volume for measured values. The data was curve fitted which is represented as estimated values in the plot. A linear relationship is found between the work function and the wear volume, which indicates no CPT at 4300 lb/ft side force for 13CrS110. This is depicted in figure 5.31.

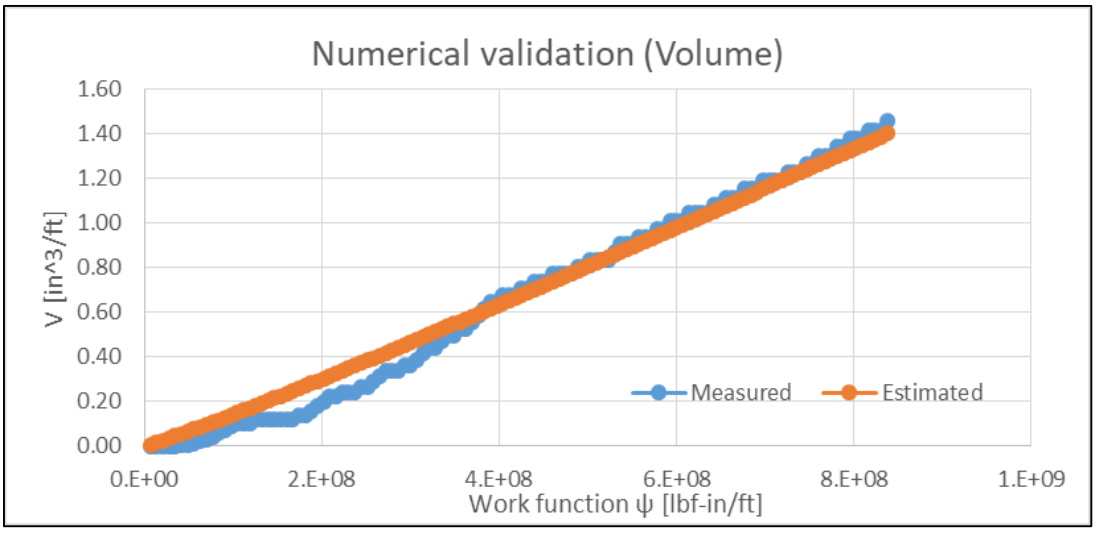

Fig 5.30: Wear volume vs Work function for 13CrS110 at 4300 lb/ft

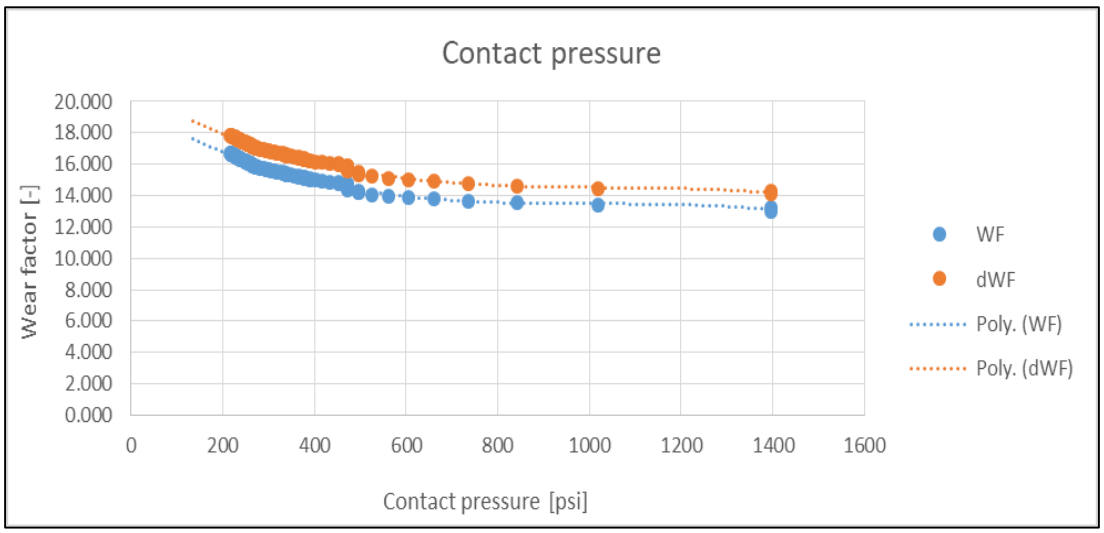

Fig 5.31: Wear Factor vs Contact Pressure for 13CrS110 at 3300 lb/ft

Figure 5.28 shows the measured wear percentage as a function of time. The casing sample was worn to ~25% of original wall thickness in 2 hours. The rate of wear is less than 13Cr80 at 4300 lb/ft side force.

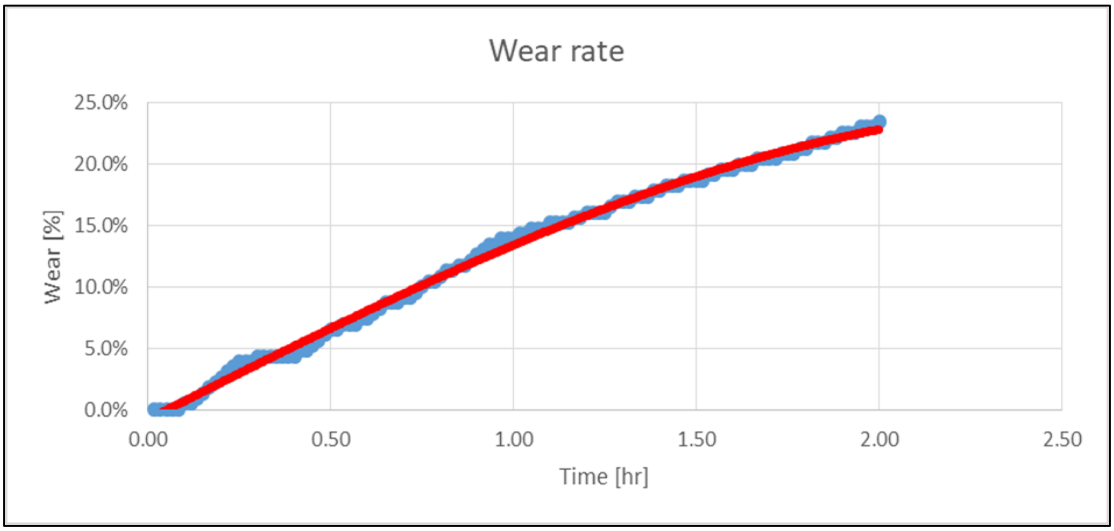

Fig 5.32: Wear rate vs Time for 13CrS110 at 4300 lb/ft

Figure 5.33 shows the wear factor against test time at 4300 lb/ft side force. There is increasing trend during the first hour of the test but later it becomes stabilize to 40 E-10 psi^{-1}. This value of WF is less than 13Cr80 at the same side force.

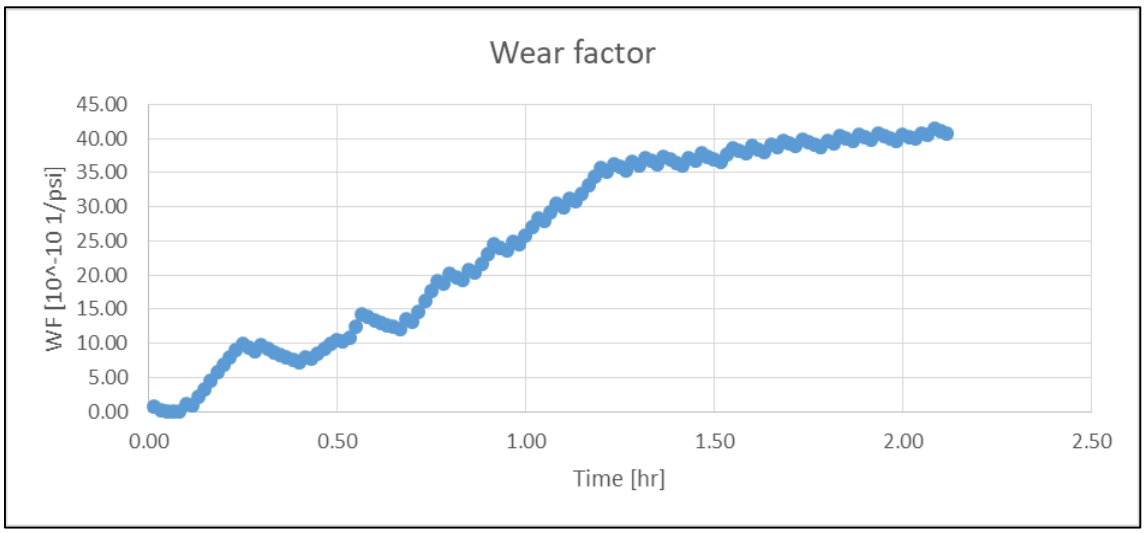

Fig 5.33: Wear Factor vs Time for 13CrS110 at 4300 lb/ft

5.9 Correction Factor

Correction factors are calculated for all tests and plotted with Mittal correction factor as illustrated in Figure 5.34. It is apparent that Test -4 on 13Cr80 and Test -5 on 13CrS110 with 650 lb/ft side force follows the trend of Mittal correction factor which indicates chrome casing exhibits wear characteristics that are similar to ordinary carbon steel only at the lower side force. The standard method for casing wear modeling can be applied to chrome material provided the side force is low. The tests indicates a CPT at 650 lb/ft side force. However, for the remaining tests, the Mittal correction factor does not provide an accurate representation of wear characteristics. The correction factors are close to one and have small deviation from unity. This indicates that the Mittal correction factor is not relevant for CRA tubulars. In order to improve the modelling of wear characteristics of CRA tubulars, the correction factor should be removed from calculations which means a linear relationship between the wear volume and the work function.

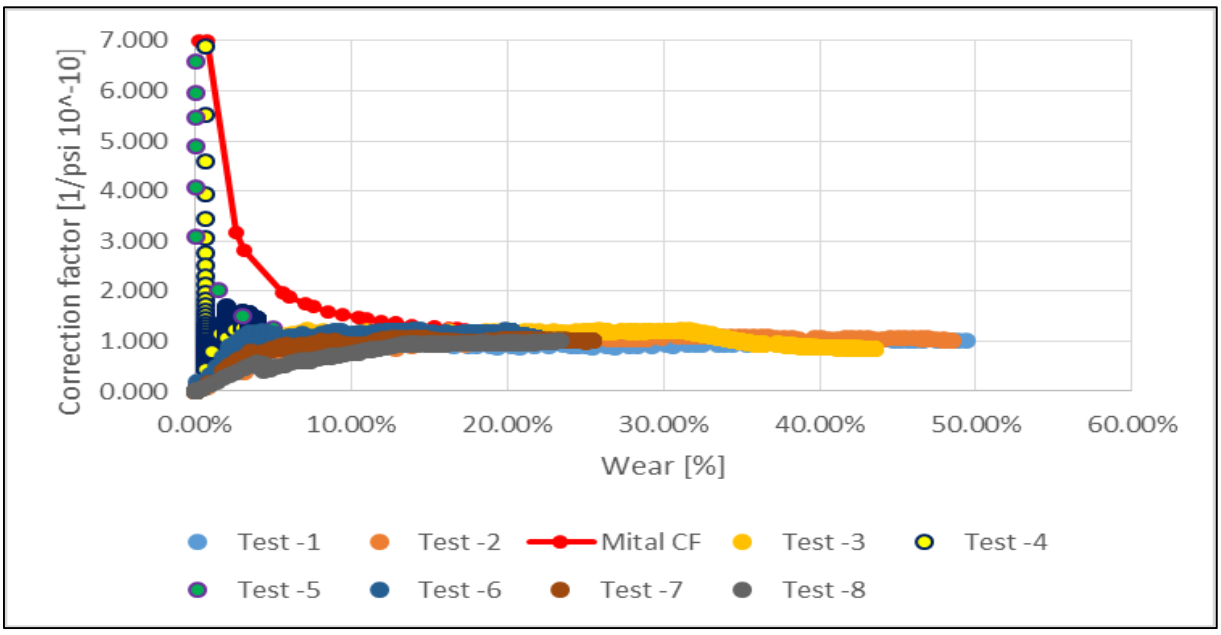

Fig 5.34: Correction Factor vs Wear percentage for CRA tubulars

5.10 Comparison between 13Cr80 and 13CrS110

Figure 5.35 shows the wear percentage against time for both 13Cr80 and 13CrS110 at 3200 lb/ft side force. It is evident that 13Cr80 is subject to significantly higher wear rate as compared to 13CrS110. A similar trend was observed for all other side forces. Figure 5.36 depicts the wear factor against side forces for both 13Cr80 and 13CrS110. The wear factors for 13CrS110 are considerably lower as compared to 13Cr80 at all side loads.

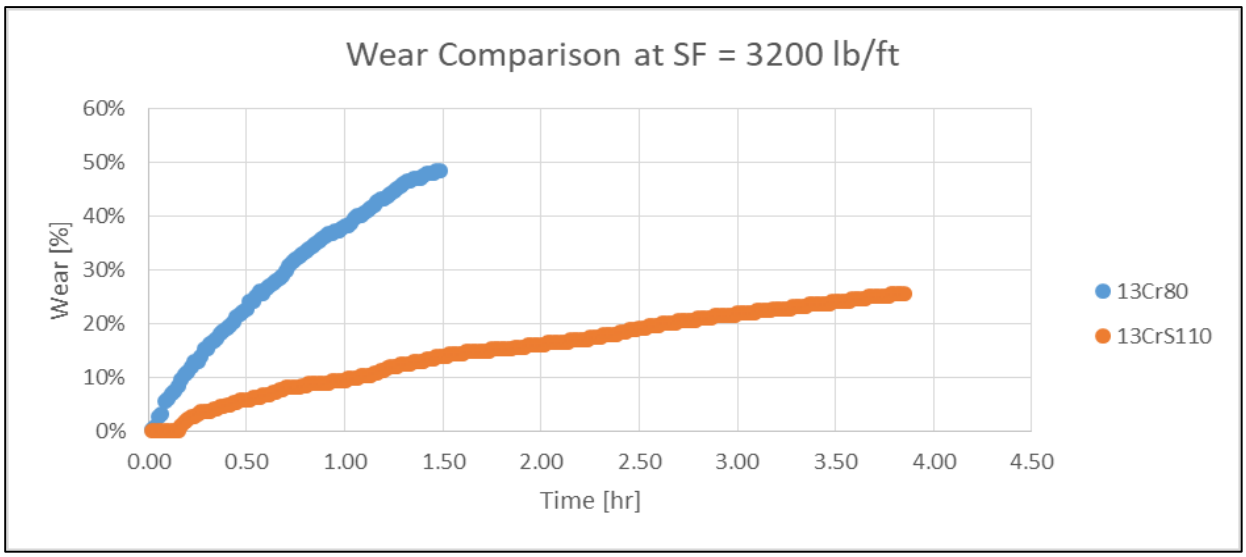

Fig 5.35: Wear percentage comparison between 13Cr80 and 13CrS110

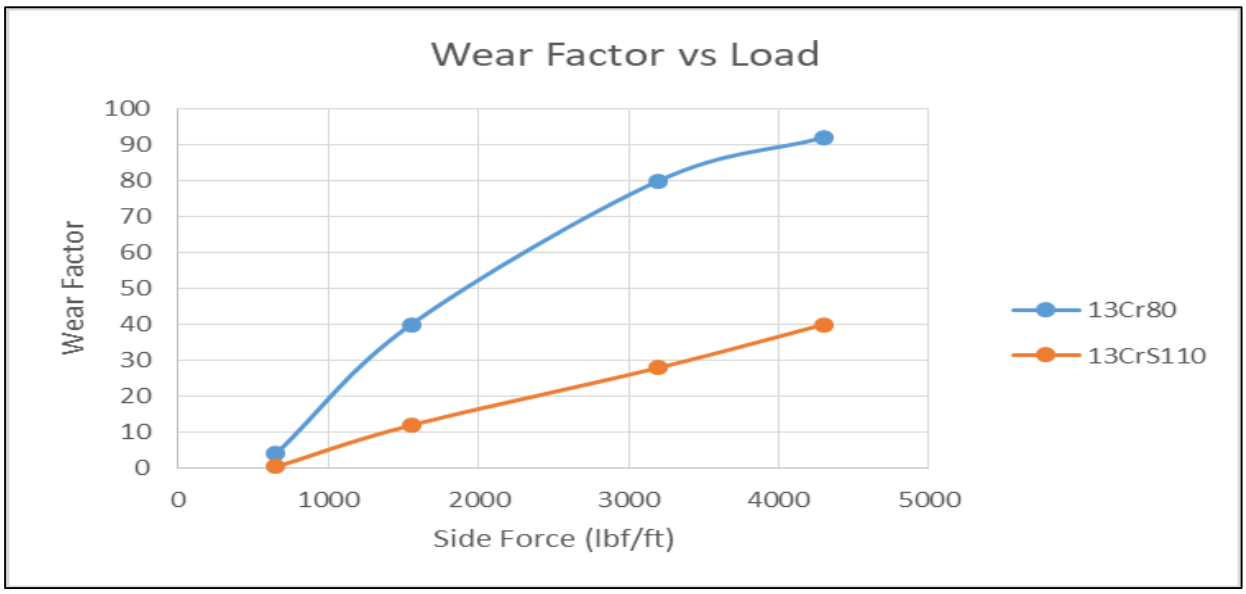

Fig 5.36: Wear factor vs Side Force

5.11 Summarized Tests Results

The summary of all the test results are presented in below table 5.1:

TEST #	MATERIAL	SIDE FORCE	DURATION	WF	CPT	WEAR
		lbf/ft	hours	E-10 psi^{-1}	psi	%
1	13Cr80	4300	1.0	90	No	50
2	13Cr80	3200	1.5	80	No	50
3	13Cr80	1550	5.0	40	40	45
4	13Cr80	650	8.0	4.0	50	4.0
5	13CrS110	650	8.0	0.50	50	1.2
6	13CrS110	1550	8.0	12	30	22
7	13CrS110	3200	4.0	28	No	25
8	13CrS110	4300	2.0	40	No	25

Table -5.1: Summarized tests results

6 Conclusion

The research conducted in this thesis was based on experience with a poor quality wear prediction for CRA materials. Data from NCS wells shows that CRA are prone to extreme rates of wear as compared to standard steel. In cooperation with industry professionals a test matrix was developed to determine the range of side forces occurring in wells where CRA are exposed to wear. The performed tests form the bases for a model that can predict wear for CRA. The findings from the laboratory testing shows the following conclusion:

- Experimental wear tests on 13Cr80 and 13CrS110 are resulted in high wear rates as compared to normal carbon steel material.
- 13CrS100 resulted in low wear and has less wear rate as compared to 13Cr80.
- At high side force, the linear wear trend for CRA has been observed and no CPT found.
- At low side force, the non-linear wear trend for CRA has been found and CPT has been established. It means that, CRA casings have similar trend as suggested by Mittal for carbon steel at low side force.
- The CPT for chrome casings exists and can be found at low side force.
- At high side force, the experimental results found that the standard casing wear modelling does not represent the wear characteristics of casings made up of CRA due to the application of correction factor. Correction factor should be omitted from modelling to improve wear estimation. It shows that casings from CRAs can be modelled and predicted for wear estimation.
- The typical range of side forces experienced in TTRD operations has been established.
- The test results in the work of Andreas Teigland are replicated and the proposed model for prediction of wear of CRA material is confirmed.

7 Further Work

The following recommendations can be addressed in future research:

- The effect of different tool joint and hard banding material can be utilized to validate the above results.
- The testing on other type of CRAs casings can be done to confirm the generalized wear characteristics.
- The further testing can be performed at low RPM to see its effect.
- The effect of Range 2 vs Range 3 drill pipe on casing wear can be investigated.

8 References

[1] - https://drillingforgas.com/technical/casing-design/corrosion-wear-fatigue/influence-of-wear-on-casing-strength.

[2] - An Experimental Study of the Wear Characteristics of Tubulars Made from Corrosion Resistant Alloys, Andreas Teigland, Sigbjørn Sangesland, Stein Inge Dale, Bjørn Brechan, Norwegian University of Science and Technology (NTNU).

[3] - Phd thesis, Andreas Teigland, Norwegian University of Science and Technology (NTNU).

[4] - Data-driven wear-factor estimation based on the inversion technique for real-time casing wear predictions, Manish K Mittal, Robello Samuel, Adolfo Gonzales, Halliburton, Italy.

[5] - Casing Wear Factors: How do They Improve Well Integrity Analyses? SPE/IADC-173053-MS, Aniket Kumar and Robello Samuel, Halliburton.

[6] - Contact Pressure Threshold: An Important New Aspect of Casing Wear, SPE 94300, Russell W. Hall, Jr., SPE, and Kenneth P. Malloy Sr., SPE.

[7] - https://www.drillingcontractor.org/dcpi/2003/dc-julyaug03/July3-TTRD.pdf

[8] - Casing Wear - Analysis of field experience and current models, master's thesis by Ingrid Solberg Kjellevoll, Norwegian university of science and technology (NTNU) June 2013.

9 Appendix

9.1 Well Trajectories & Side Forces Plot

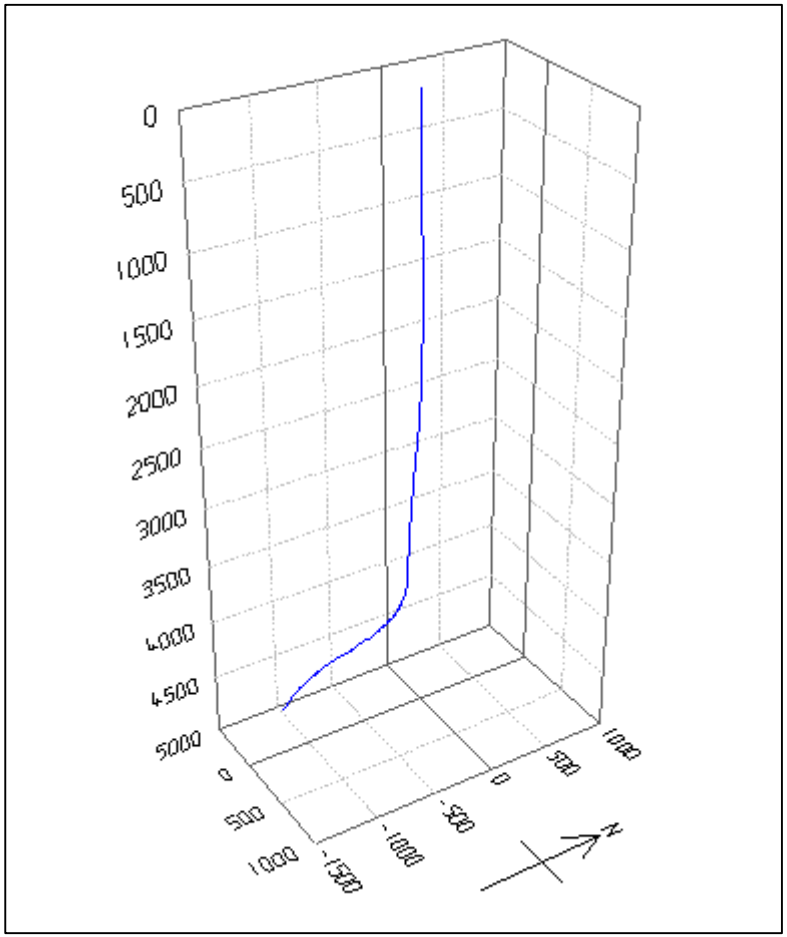

Fig 9.1: Well trajectory for well B

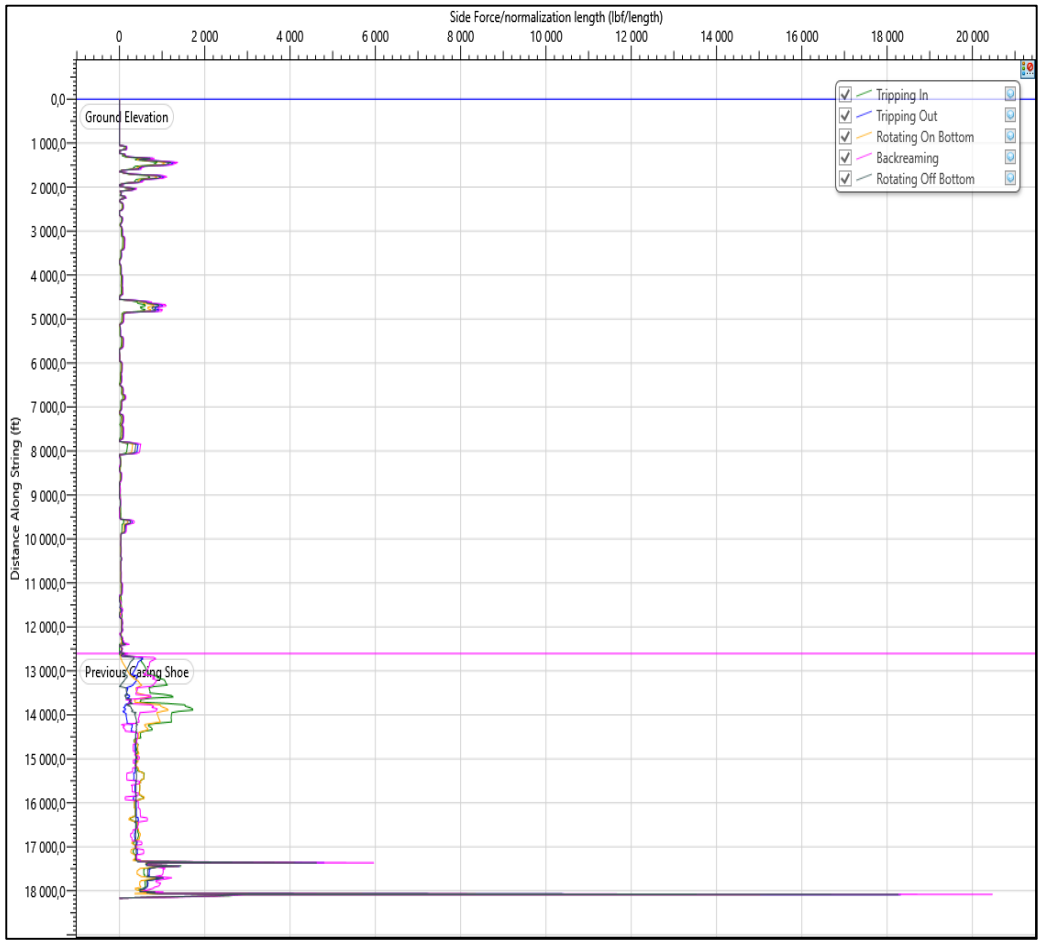

Fig 9.2: Side force plot for well B

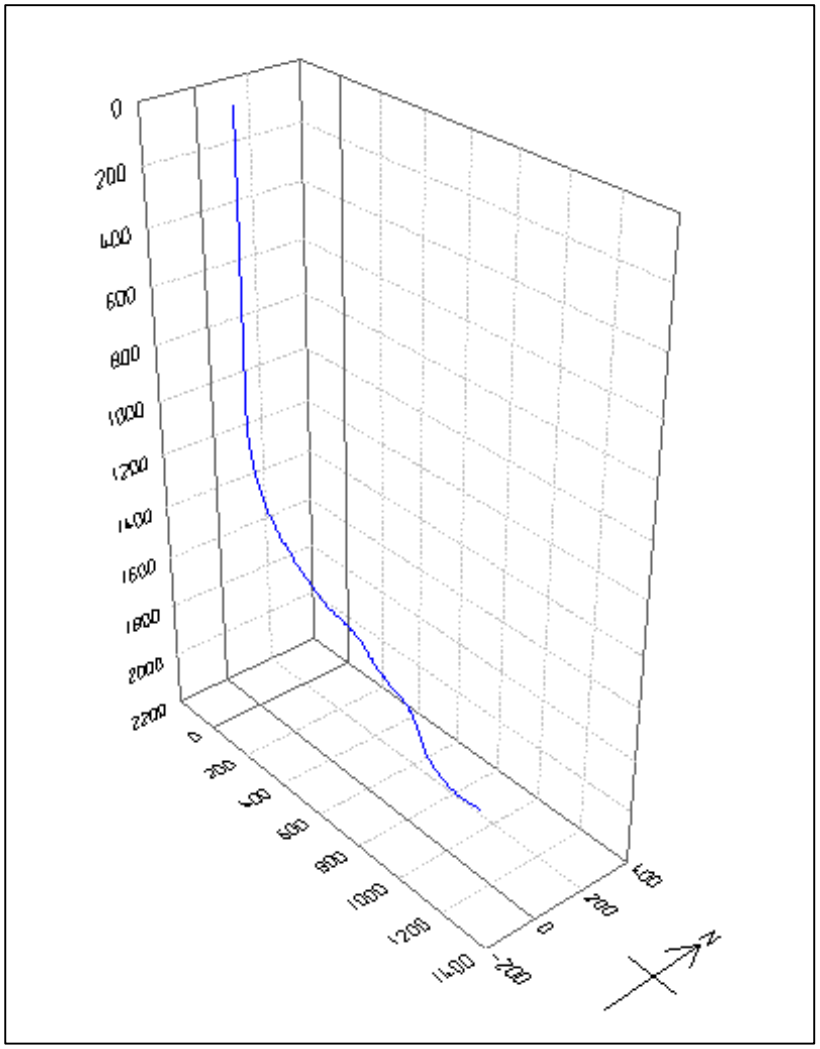

Fig 9.3: Well trajectory for well C

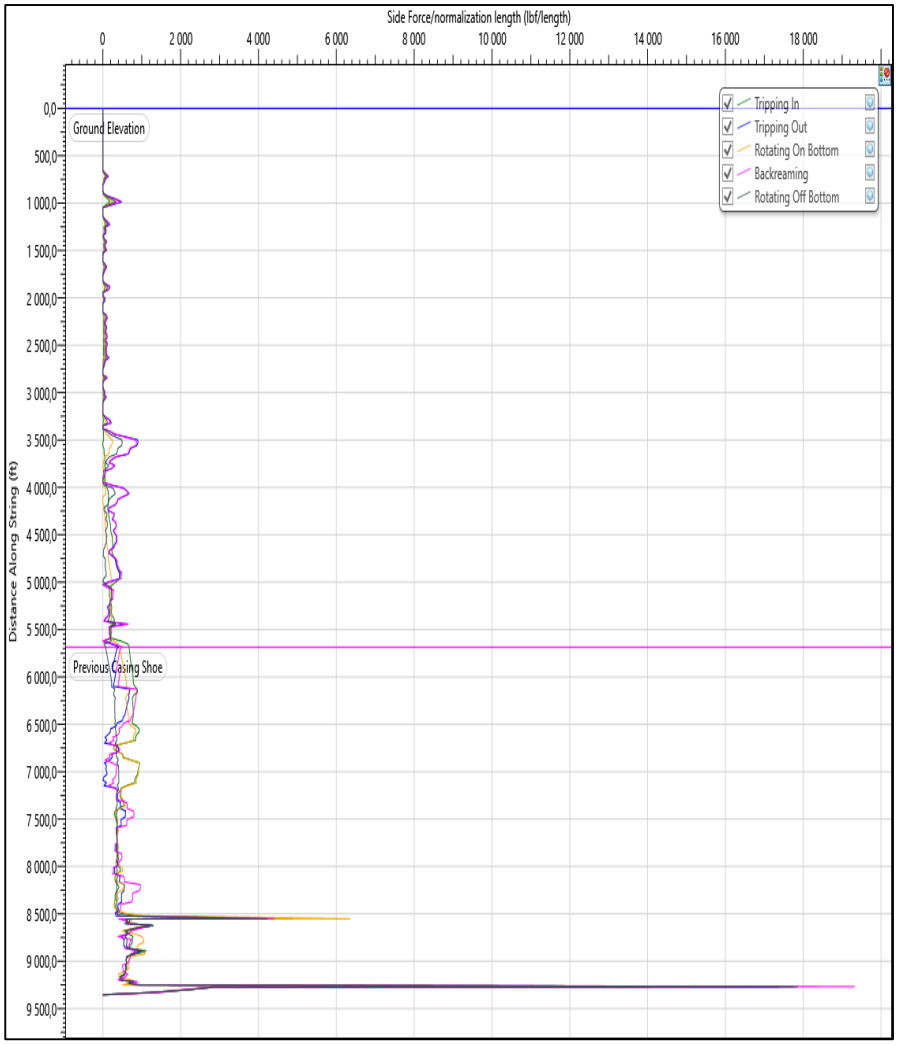

Fig 9.4: Side force plot for well C

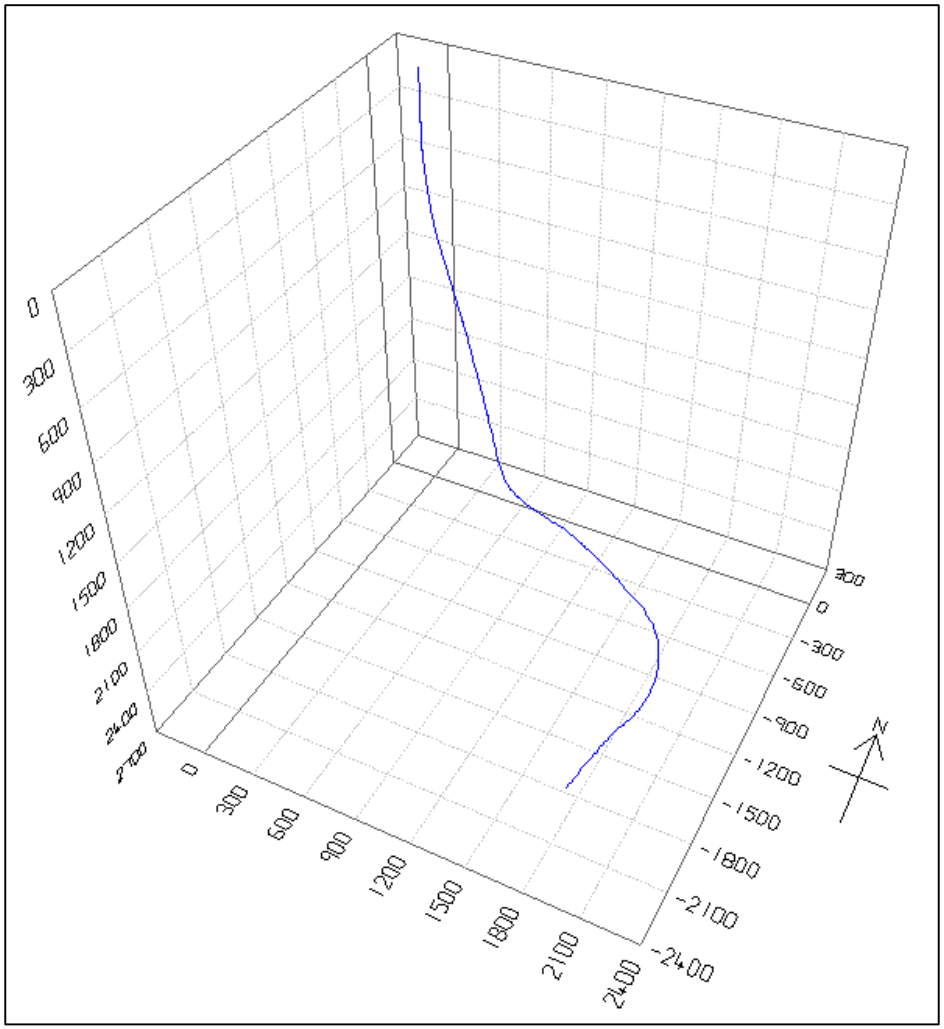

Fig 9.5: Well trajectory for well D

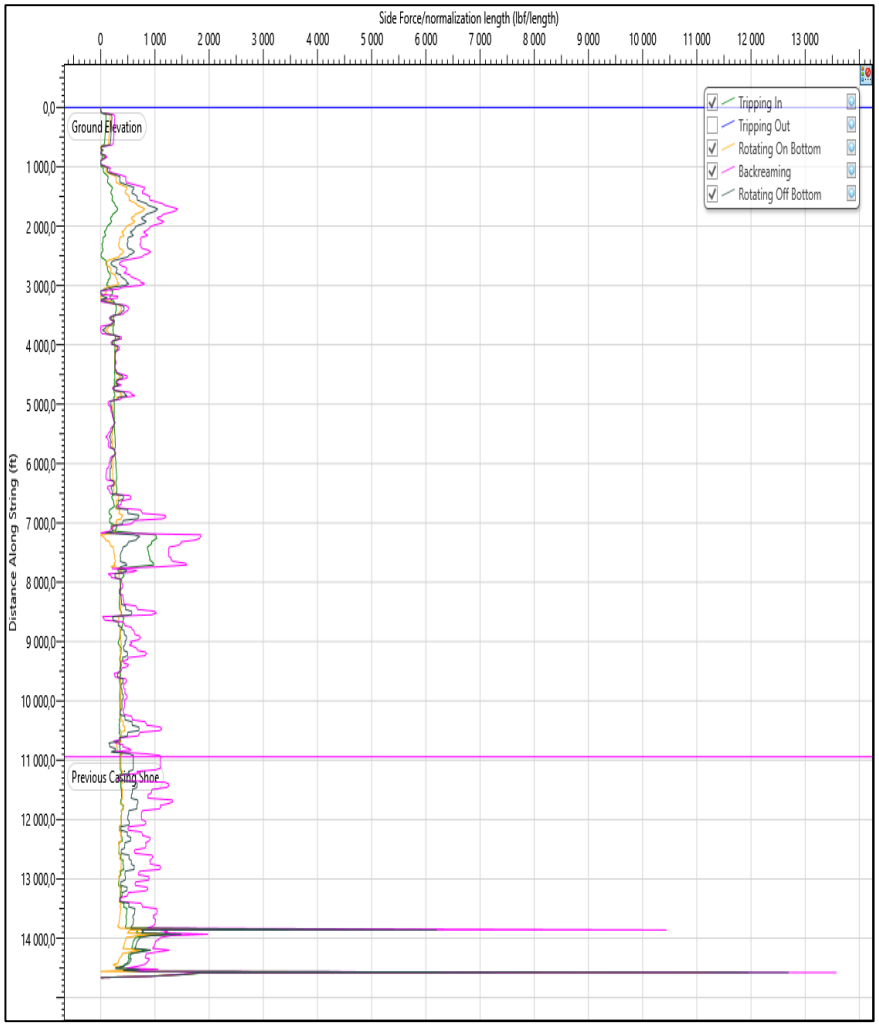

Fig 9.6: Side force plot for well D

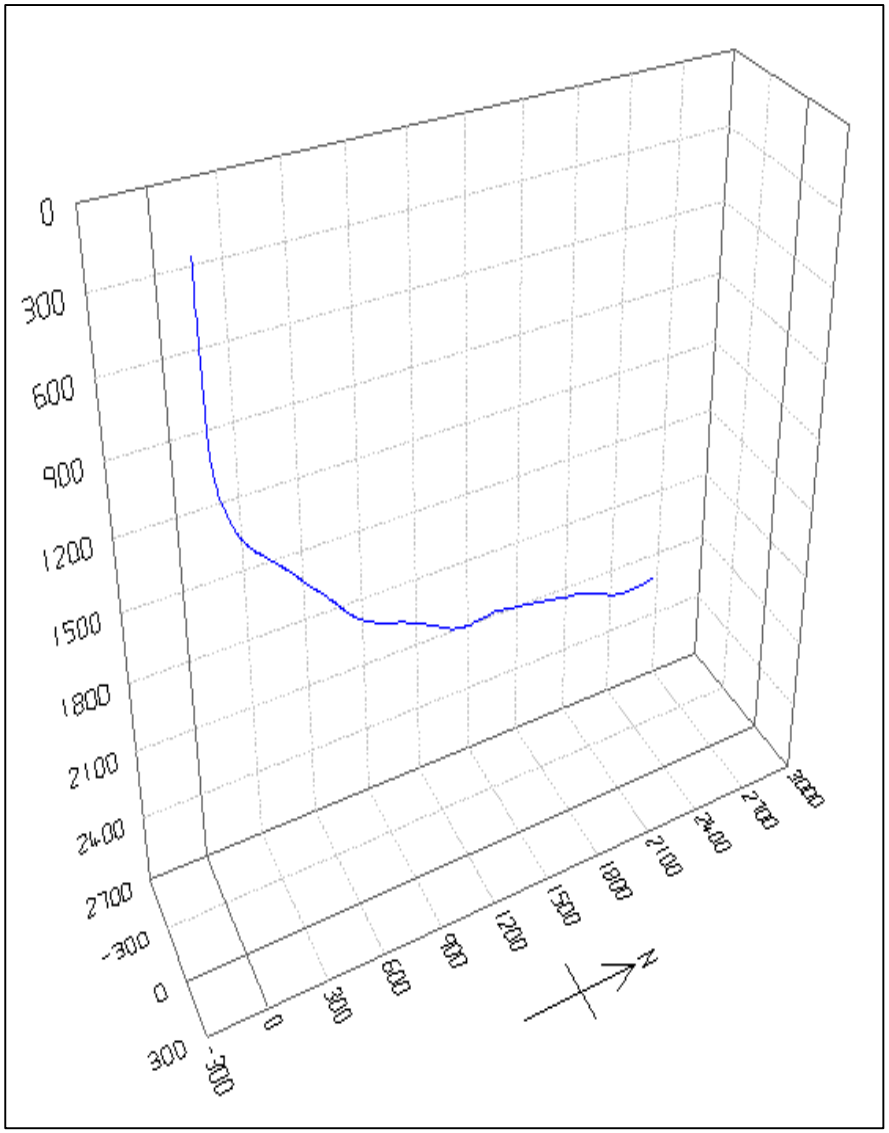

Fig 9.7: Well trajectory for well E

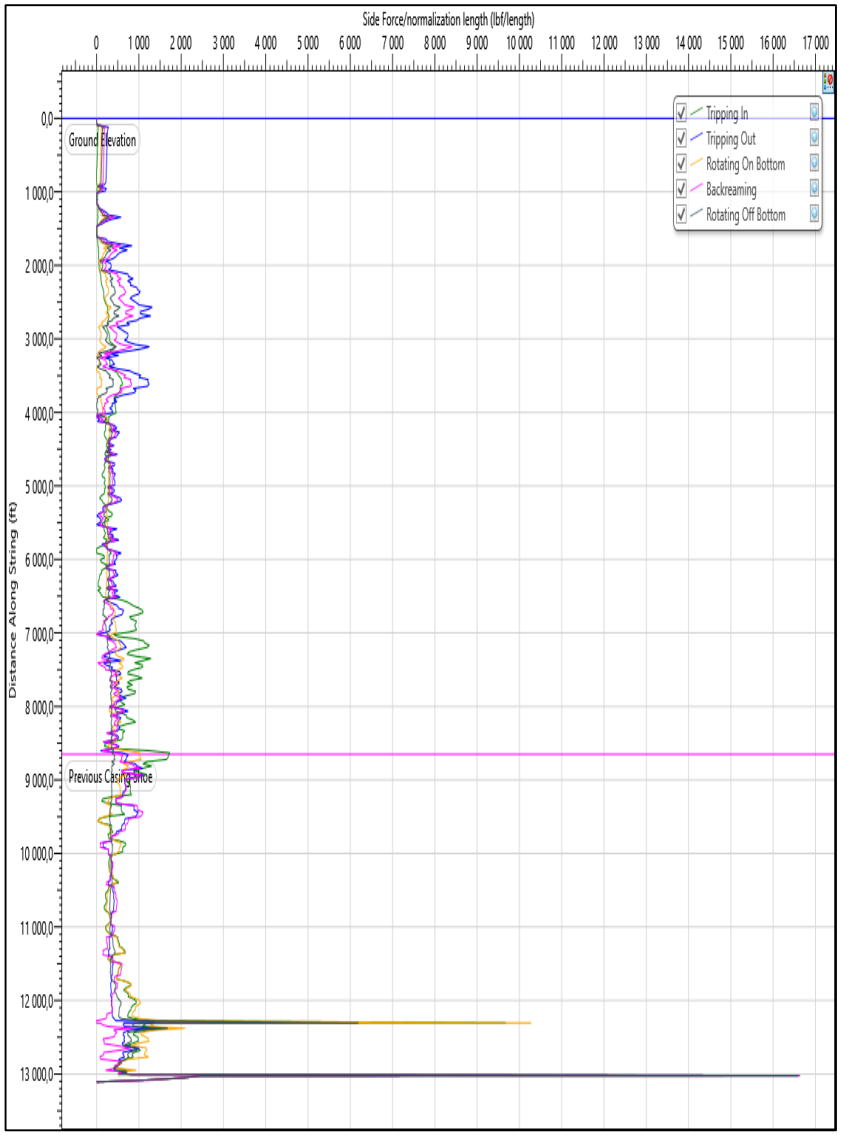

Fig 9.8: Side force plot for well E

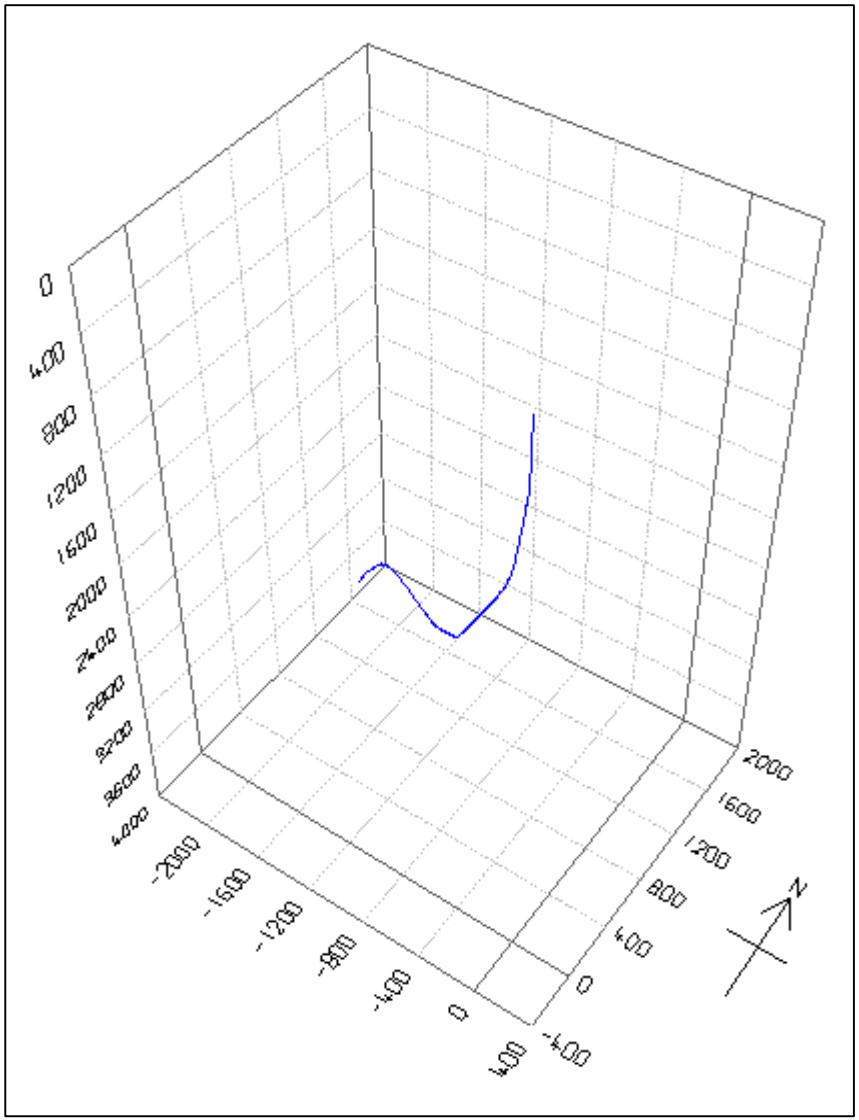

Fig 9.9: Well trajectory for well F

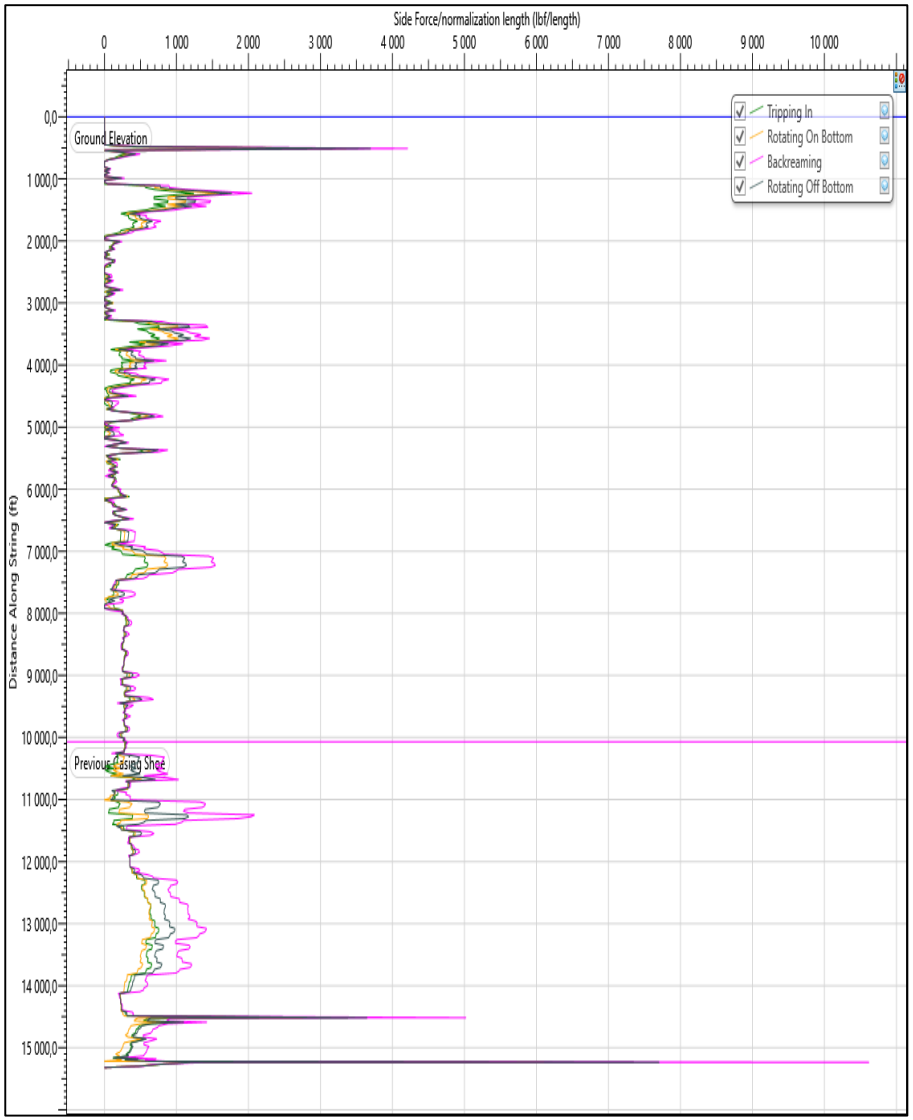

Fig 9.10: Side force plot for well F

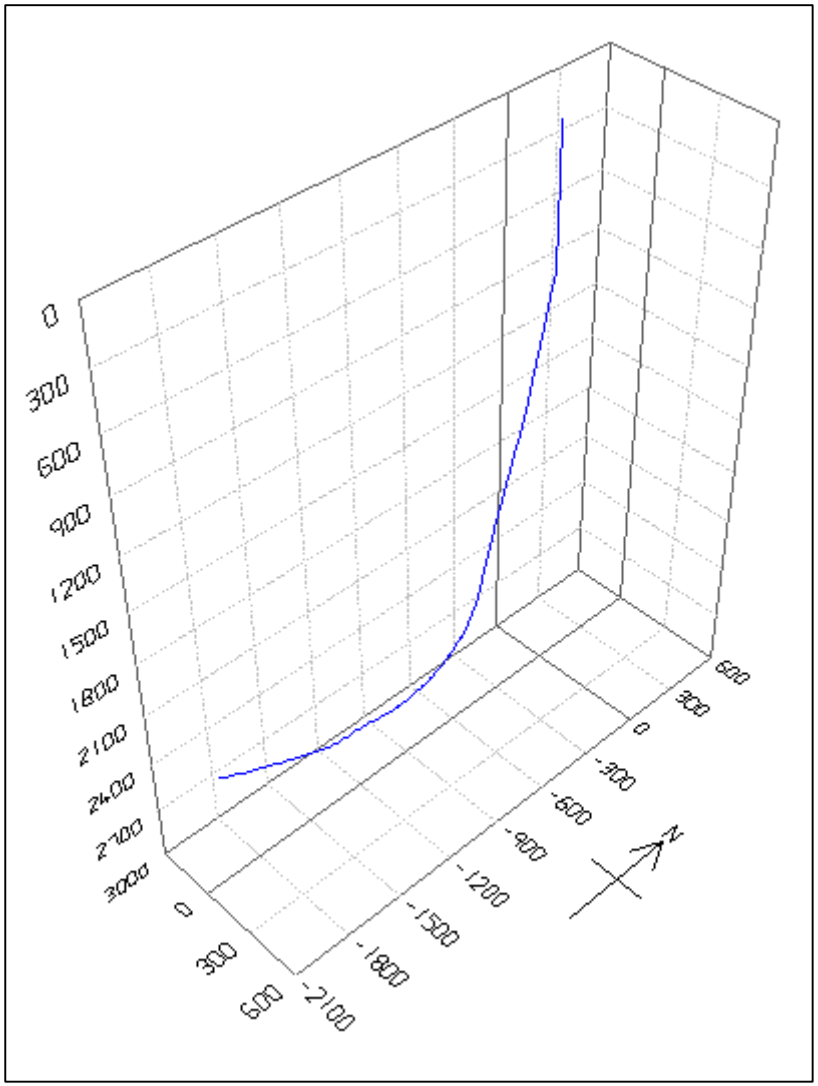

Fig 9.11: Well trajectory for well G

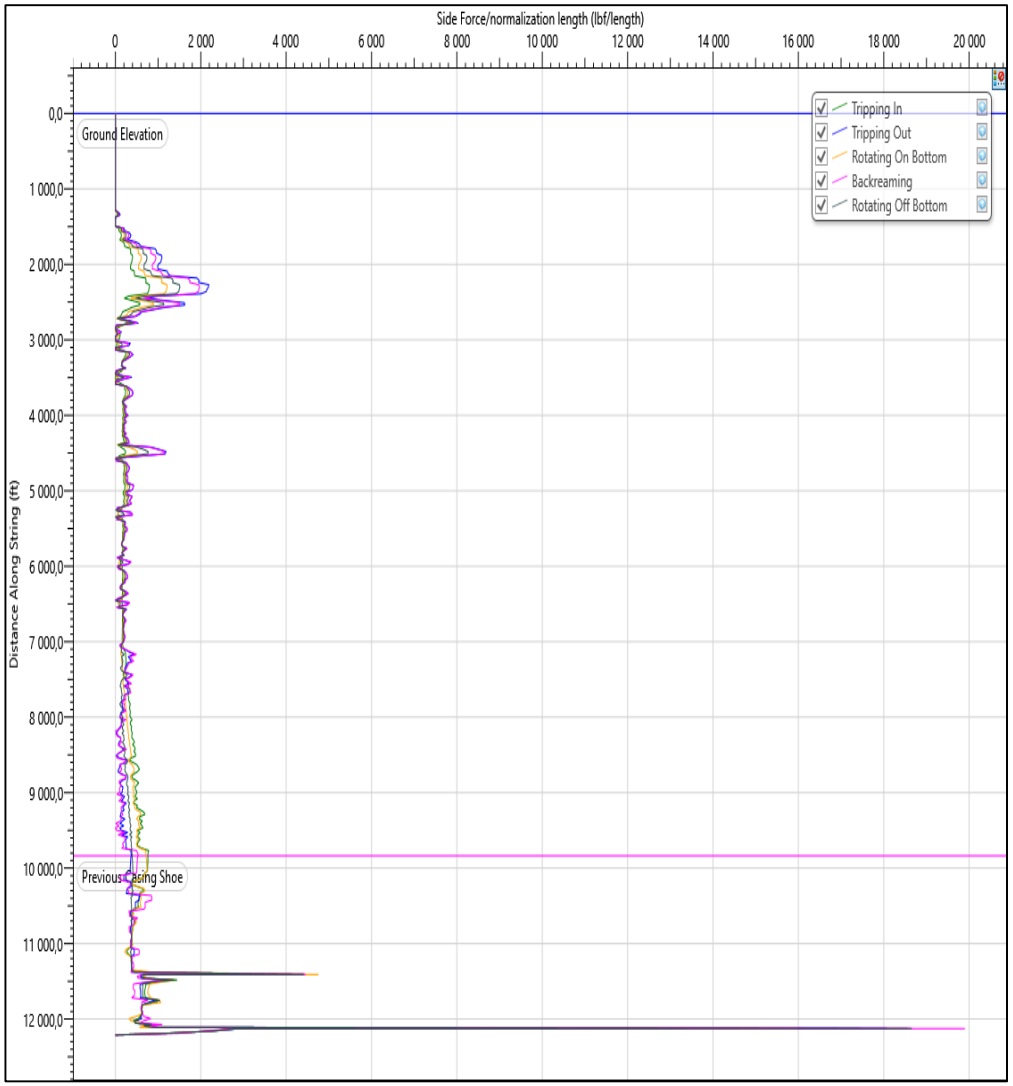

Fig 9.12: Side force plot for well G

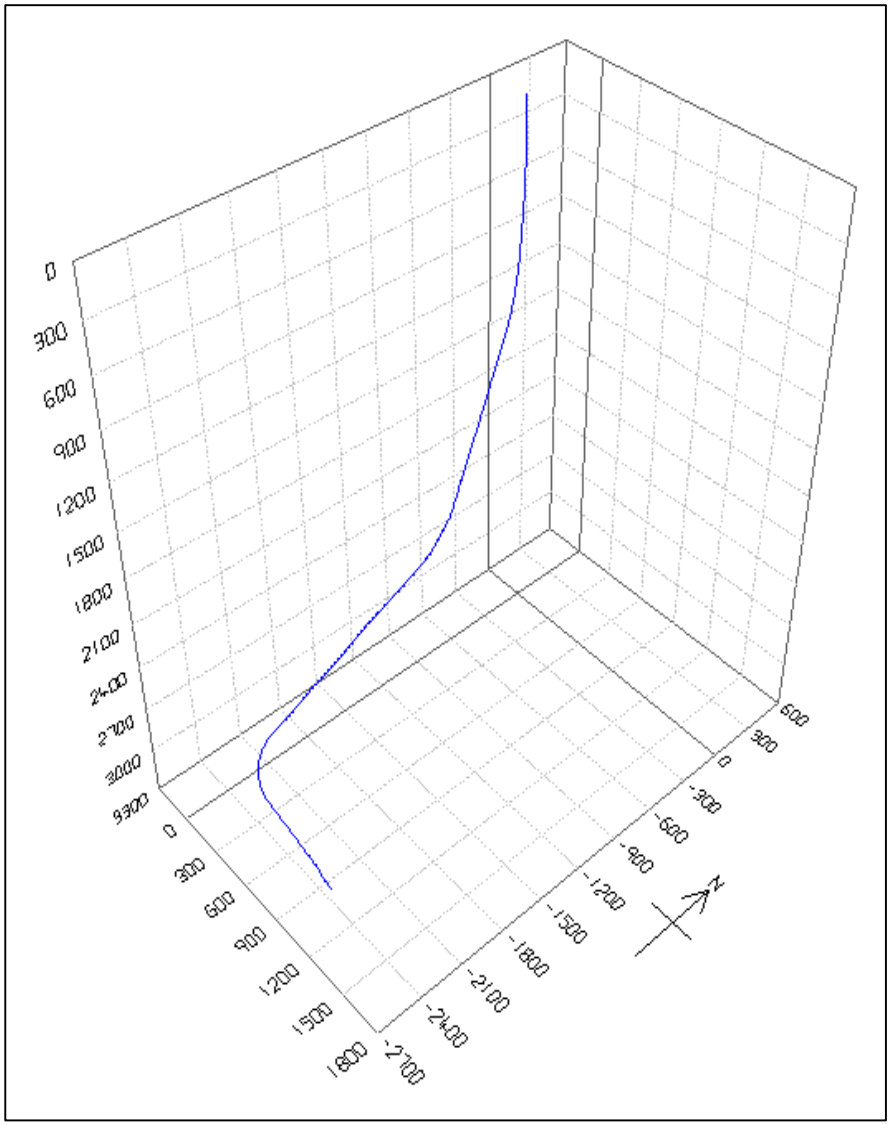

Fig 9.13: Well trajectory for well H

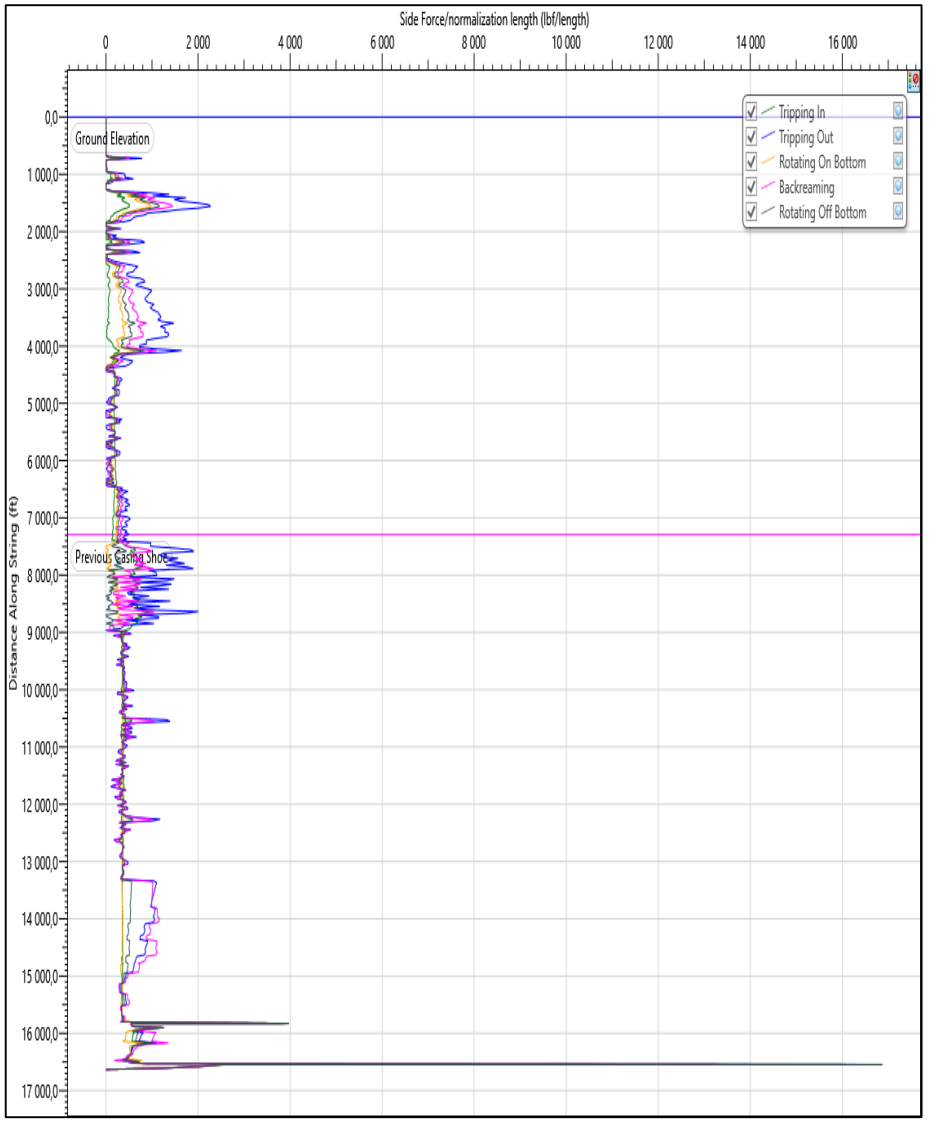

Fig 9.14: Side force plot for well H

9.2 Test -1: 13Cr80 with Side Force = 4300 lb/ft Plots

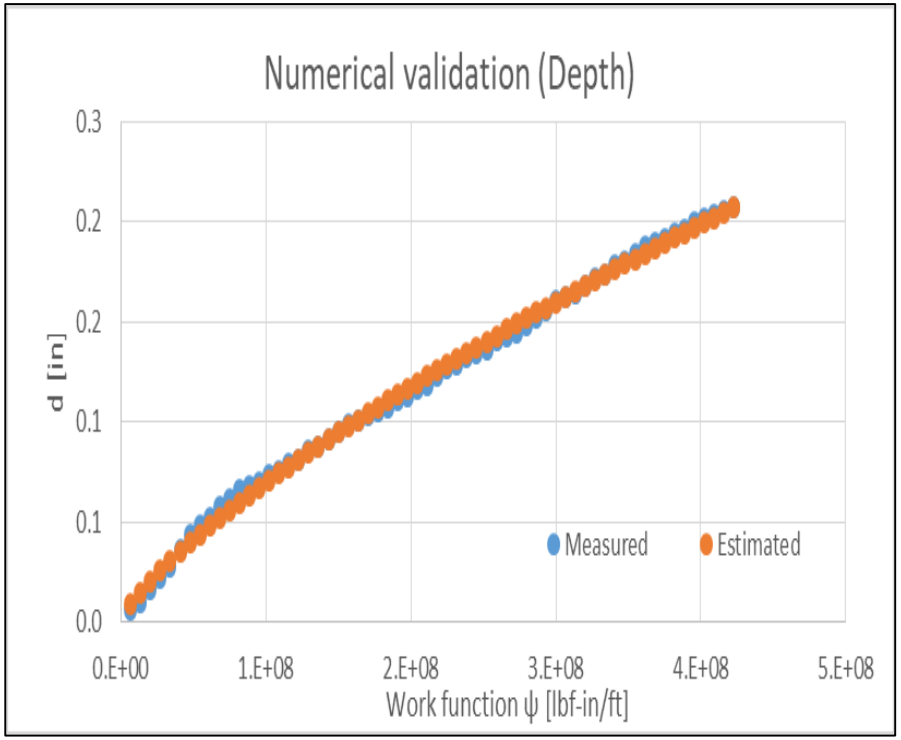

Fig 9.15: Wear depth vs Work function for 13Cr80 at 4300 lb/ft

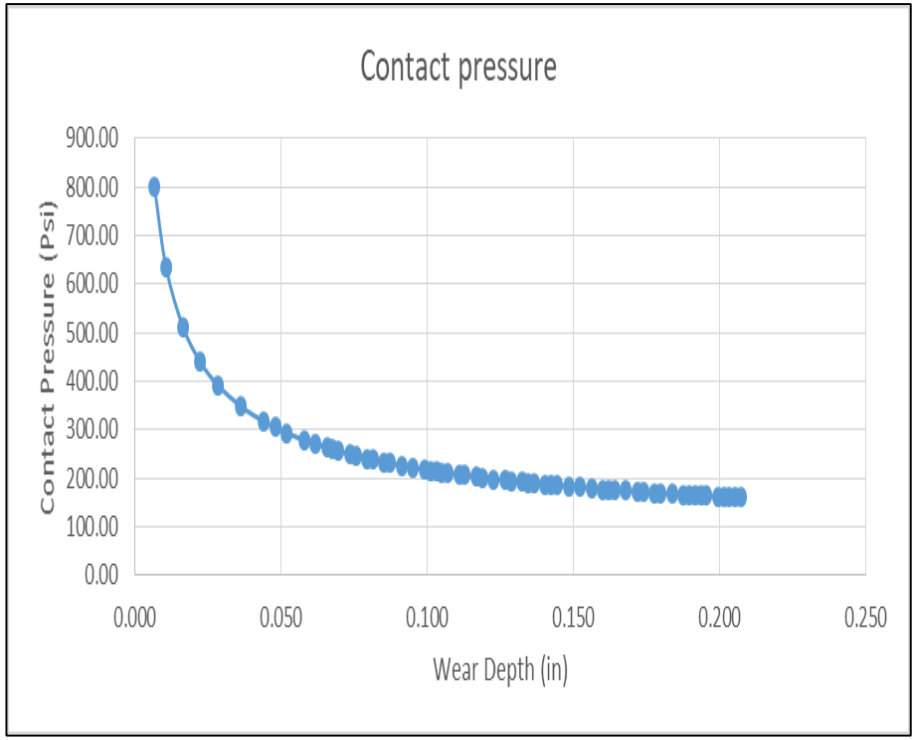

Fig 9.16: Contact pressure vs Wear depth for 13Cr80 at 4300 lb/ft

9.3 Test -2: 13Cr80 with Side Force = 3200 lb/ft Plots

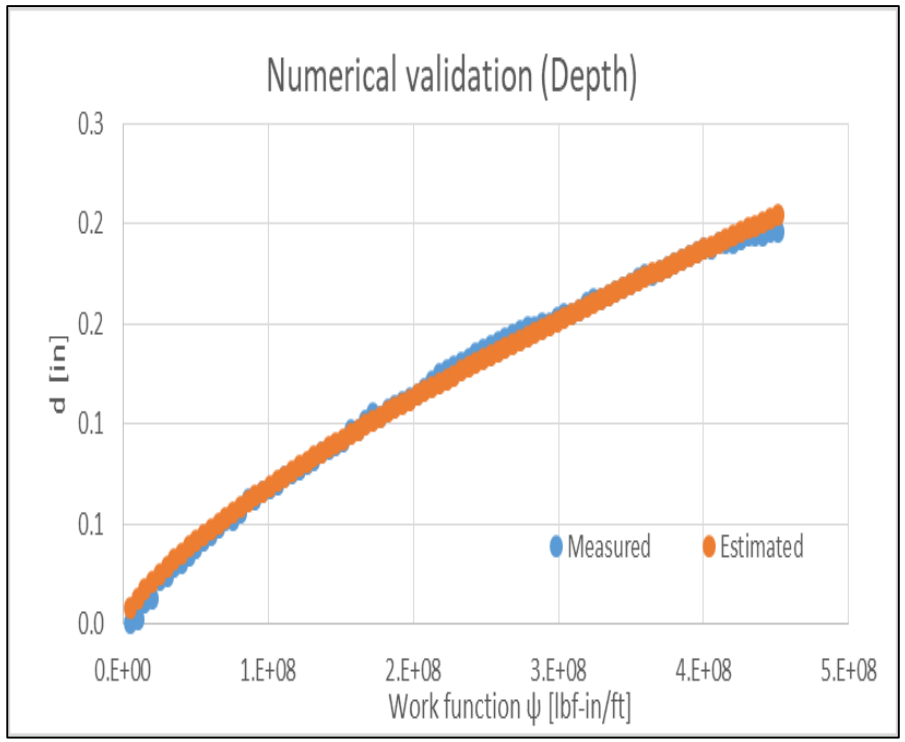

Fig 9.17: Wear depth vs Work function for 13Cr80 at 3200 lb/ft

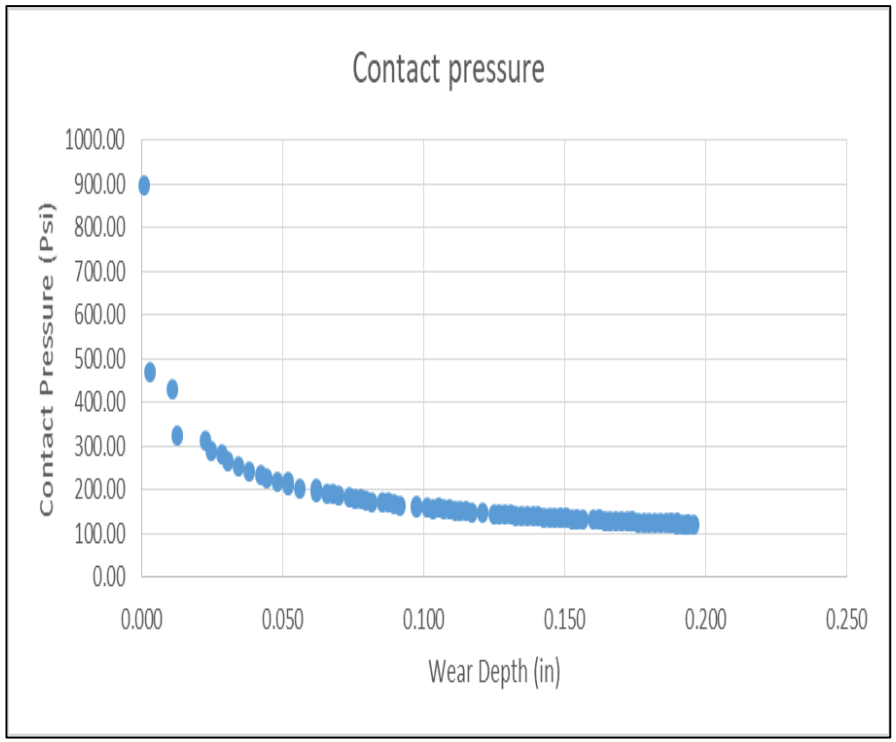

Fig 9.18: Contact pressure vs Wear depth for 13Cr80 at 3200 lb/ft

9.4 Test -3: 13Cr80 with Side Force = 1550 lb/ft Plots

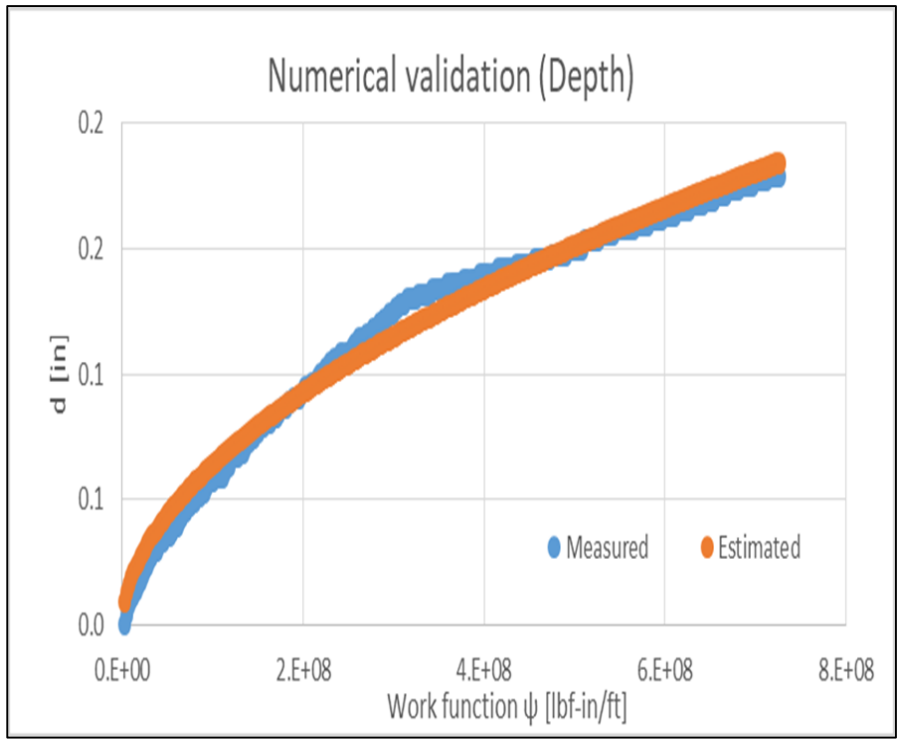

Fig 9.19: Wear depth vs Work function for 13Cr80 at 1550 lb/ft

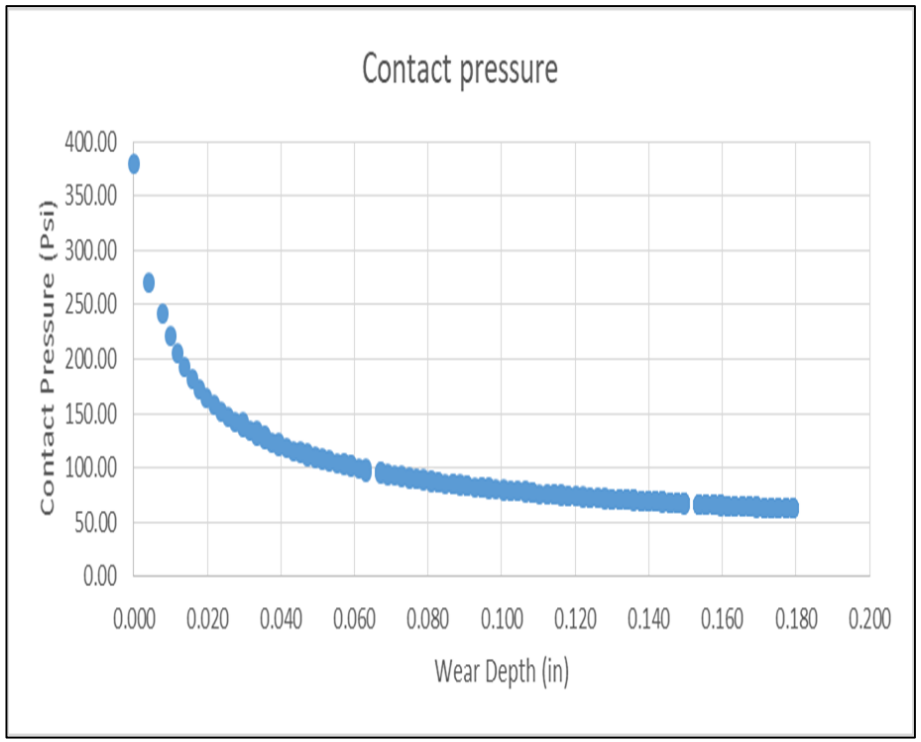

Fig 9.20: Contact pressure vs Wear depth for 13Cr80 at 1550 lb/ft

9.5 Test -4: 13Cr80 with Side Force = 650 lb/ft Plots

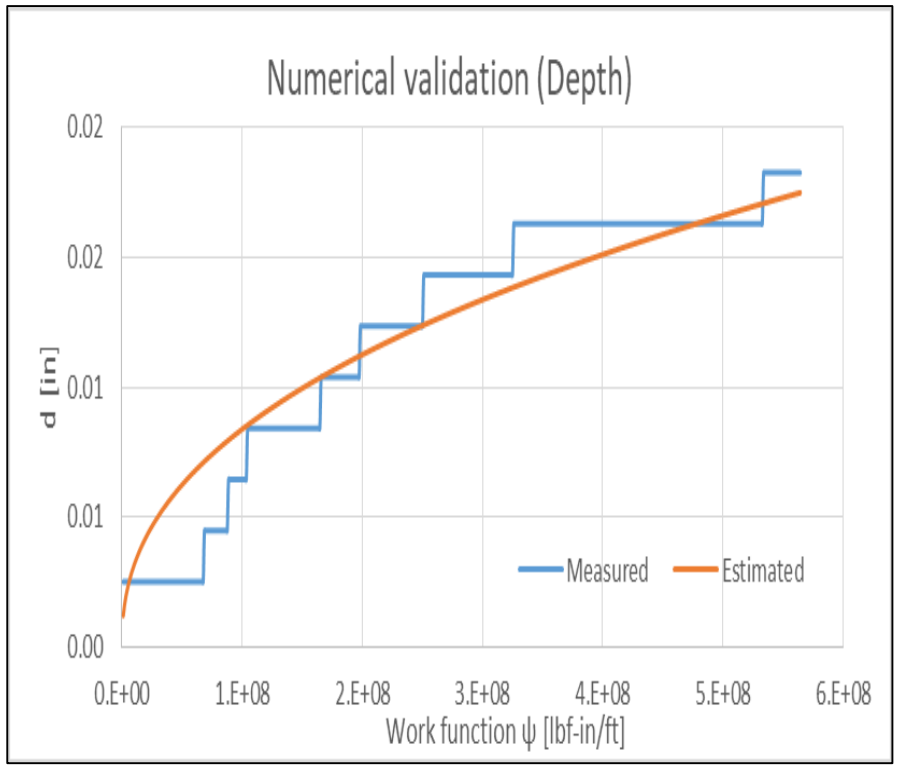

Fig 9.21: Wear depth vs Work function for 13Cr80 at 650 lb/ft

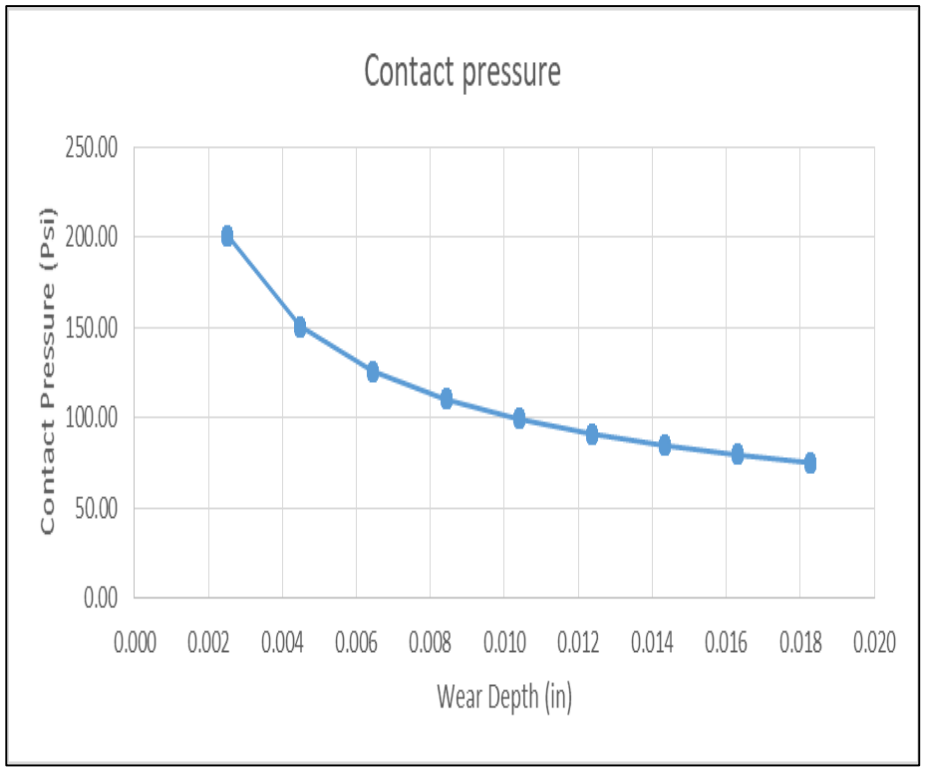

Fig 9.22: Contact pressure vs Wear depth for 13Cr80 at 650 lb/ft

9.6 Test -5: 13CrS110 with Side Force = 650 lb/ft Plots

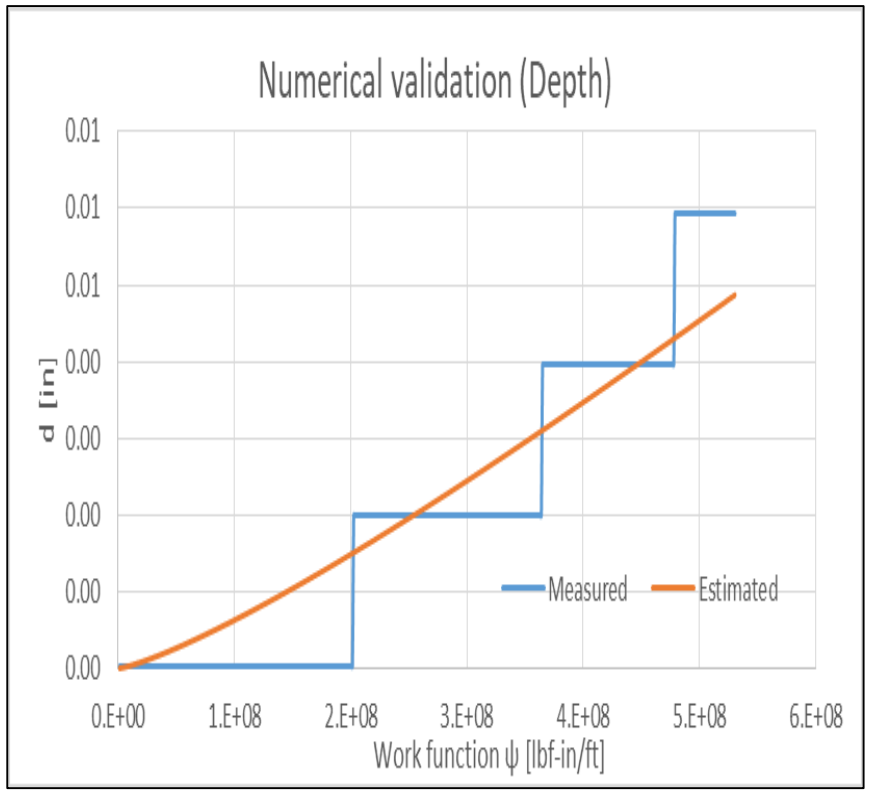

Fig 9.23: Wear depth vs Work function for 13CrS110 at 650 lb/ft

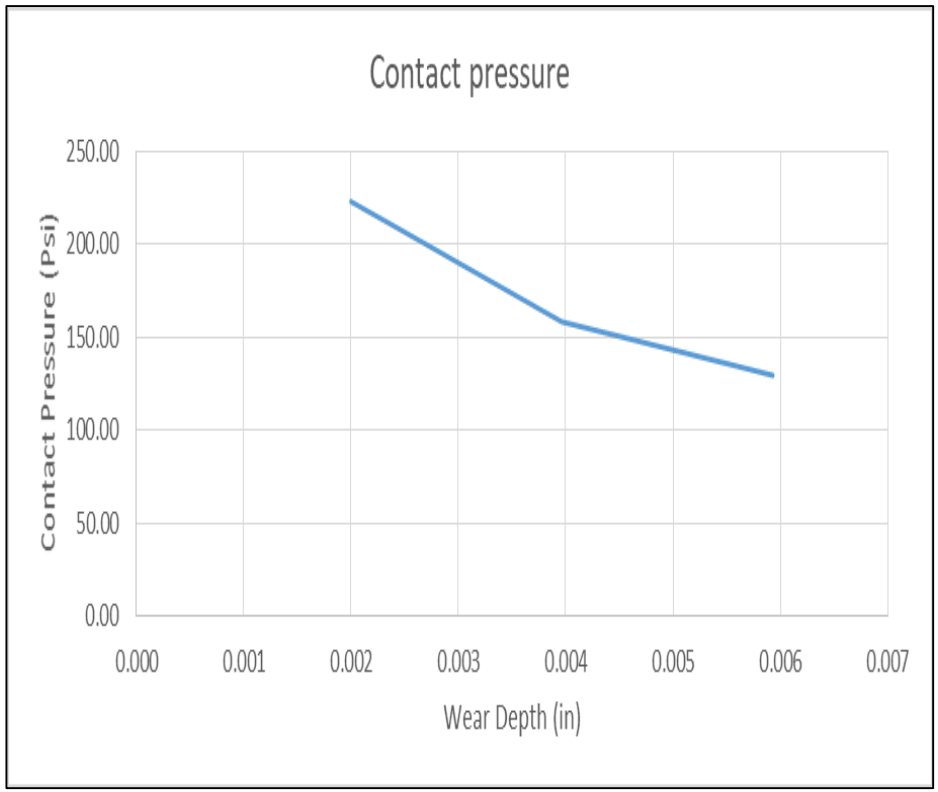

Fig 9.24: Contact pressure vs Wear depth for 13CrS110 at 650 lb/ft

9.7 Test -6: 13CrS110 with Side Force = 1550 lb/ft Plots

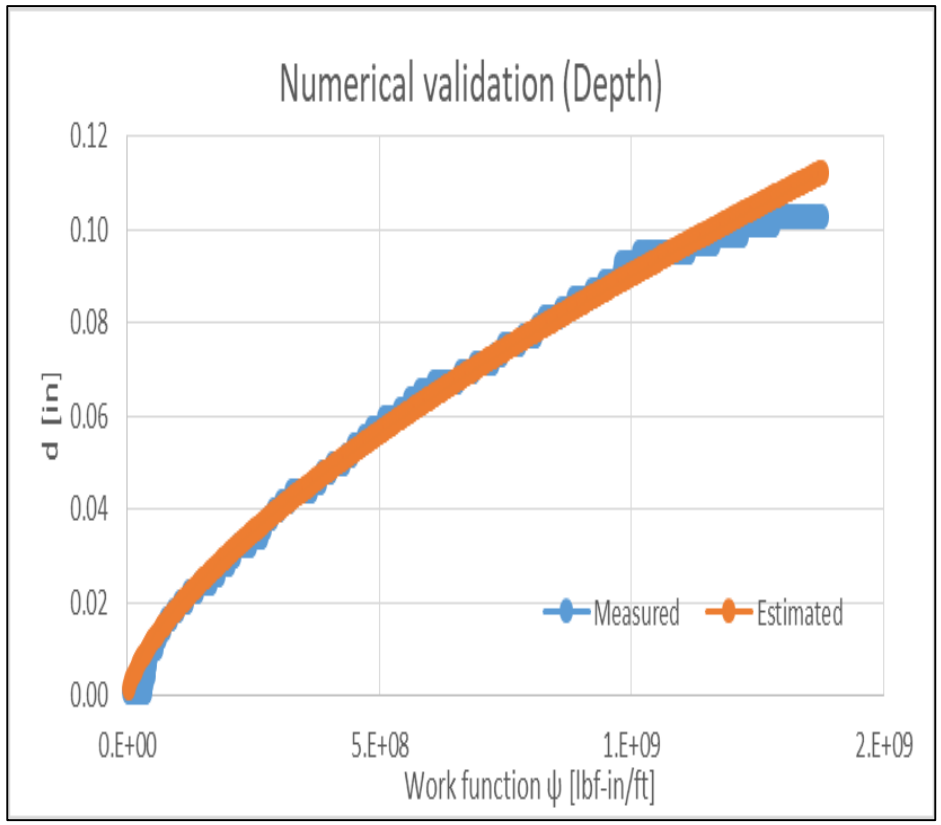

Fig 9.23: Wear depth vs Work function for 13CrS110 at 1550 lb/ft

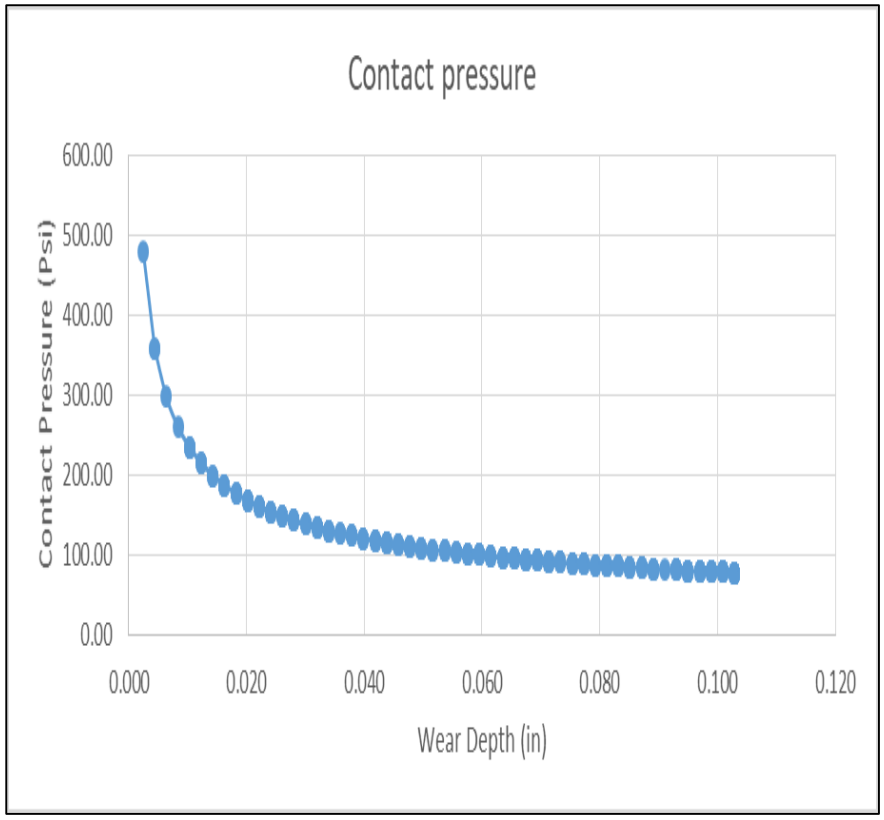

Fig 9.24: Contact pressure vs Wear depth for 13CrS110 at 1550 lb/ft

9.8 Test -7: 13CrS110 with Side Force = 3200 lb/ft Plots

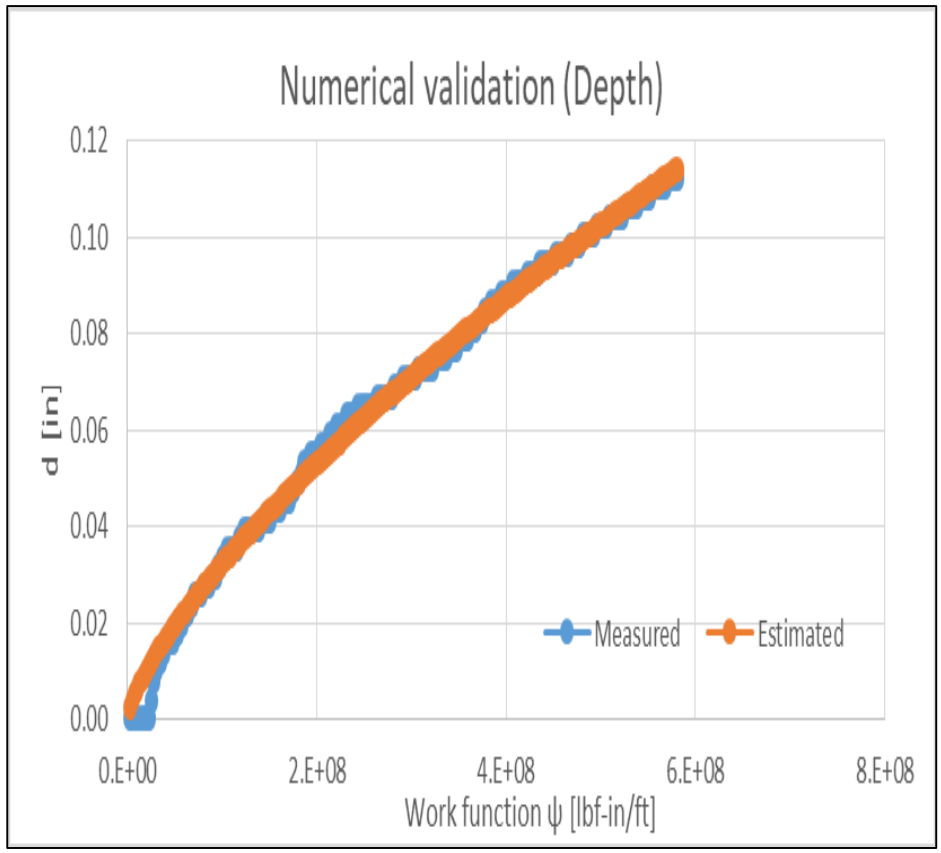

Fig 9.25: Wear depth vs Work function for 13CrS110 at 3200 lb/ft

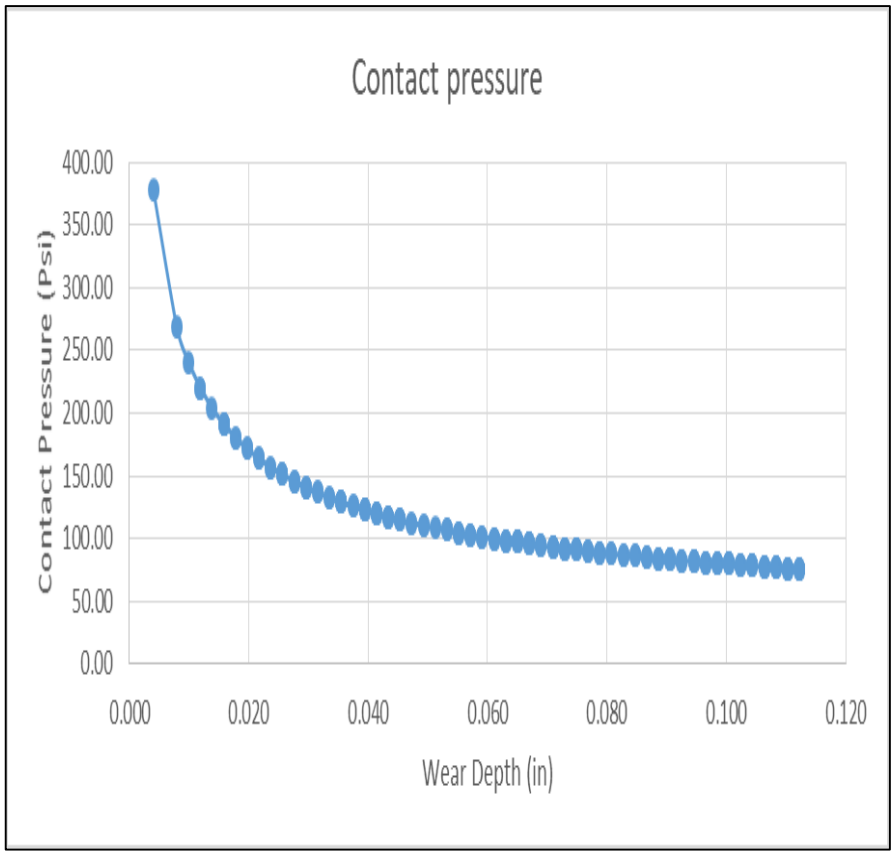

Fig 9.26: Contact pressure vs Wear depth for 13CrS110 at 3200 lb/ft

9.9 Test -8: 13CrS110 with Side Force = 3200 lb/ft Plots

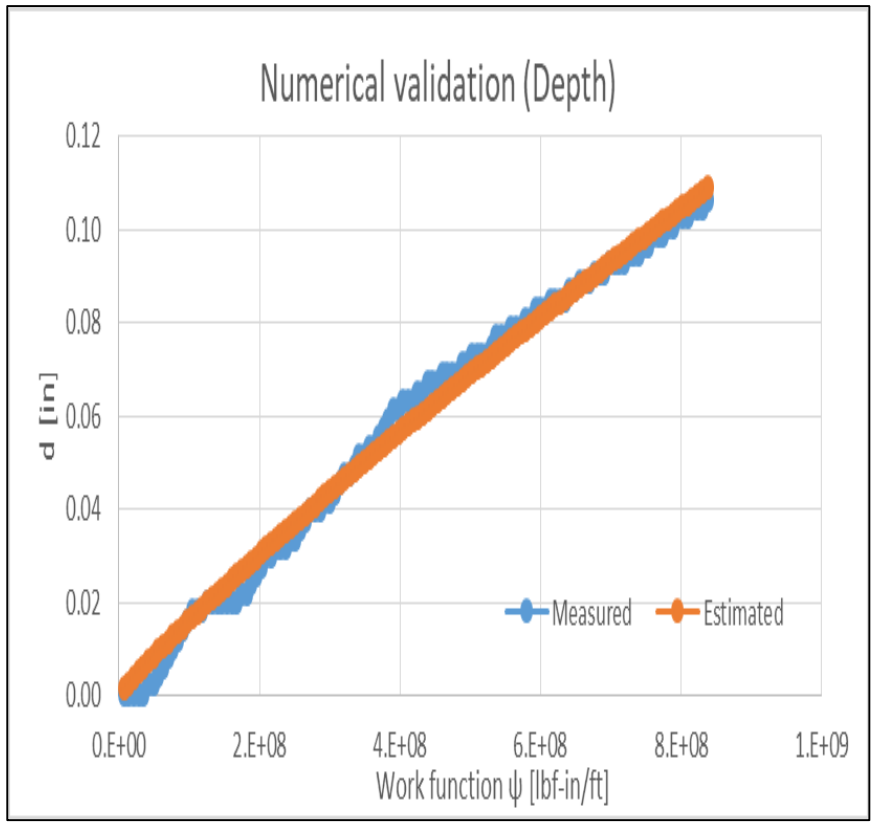

Fig 9.27: Wear depth vs Work function for 13CrS110 at 4300 lb/ft

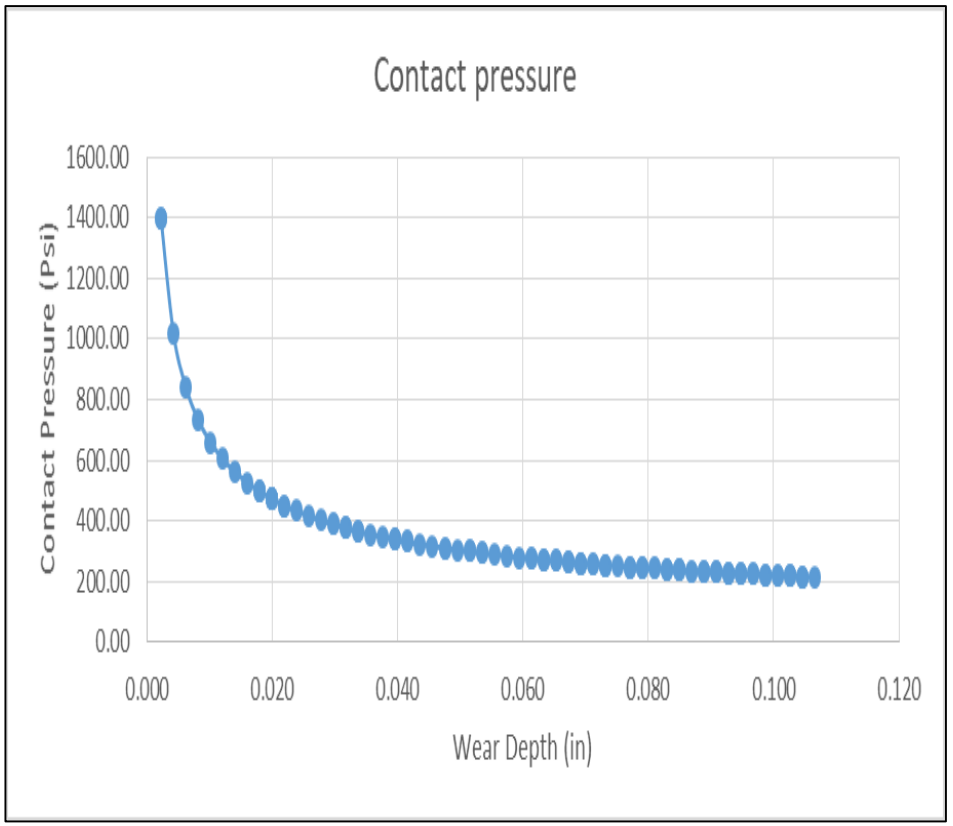

Fig 9.28: Contact pressure vs Wear depth for 13CrS110 at 4300 lb/ft

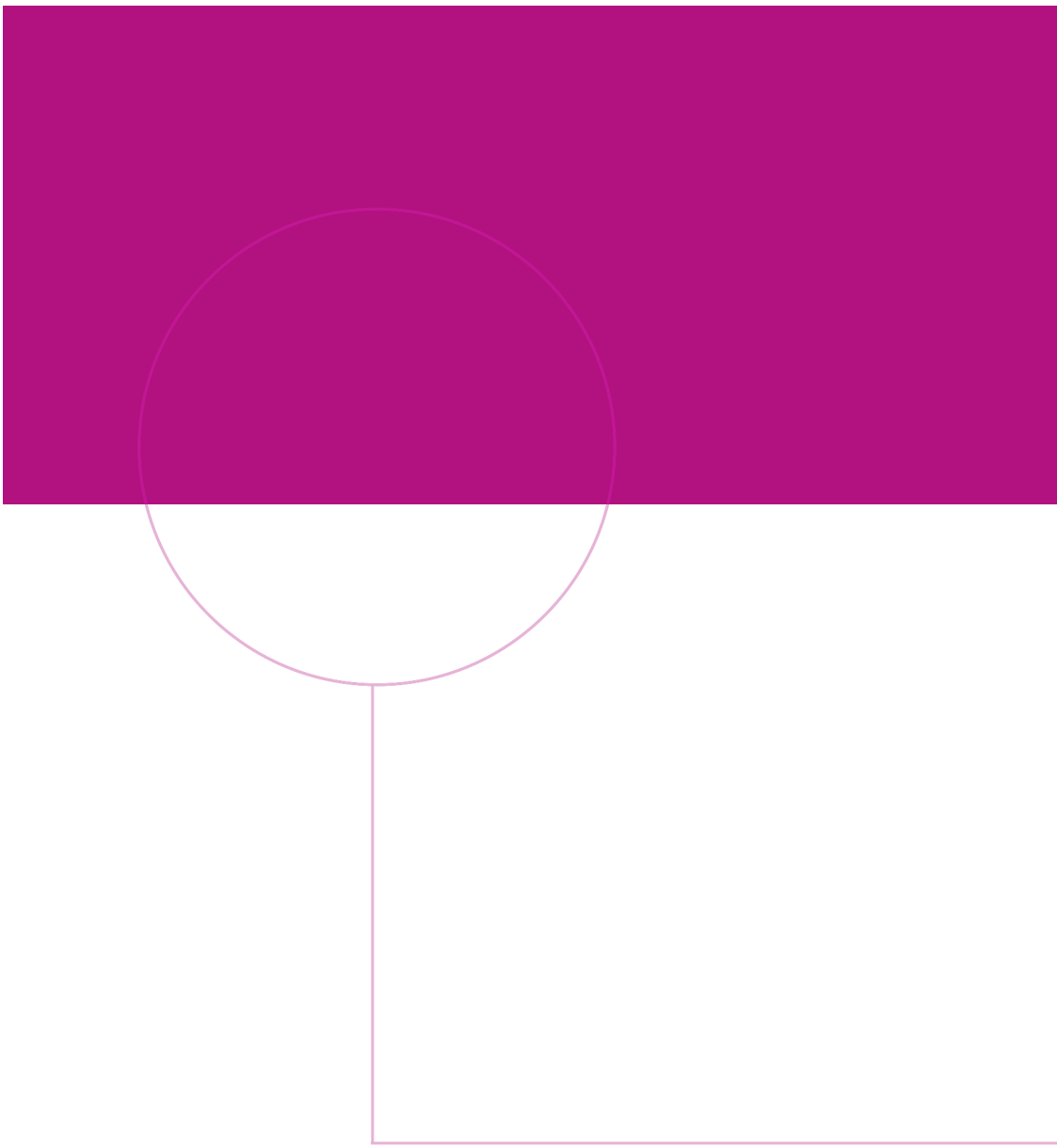

NTNU

Norwegian University of
Science and Technology